Single-cell characterization of skin response to a bite by West Nile virus-infected mosquito reveals fibroblast-mediated barrier to transmission

Hacène Medkour[1*], Federico Bocci[2*], Norman Schneider[1], Idalba Serrato-Pomar[1], Félix Rey-Cadilhac[1], Elliott F. Miot[1], Wilfried Saron[3], Ashley St John[3], Ghizlane Maarifi[4], Yingzi Liu[5], Dorothée Missé[1], Qing Nie[5,6], Duncan R. Smith[7], Sébastien Nisole[4,8], Maksim V. Plikus[5,#], Julien Pompon[1,7,#,¶]

1 MIVEGEC, University Montpellier, IRD, CNRS, Montpellier, France

2 Radboud institute for molecular life sciences, Radboud University, Nijmegen, Netherlands

3 Program in Emerging Infectious Diseases, Duke-NUS Medical School, Singapore.

4 Institut de Recherche en Infectiologie de Montpellier (IRIM), Univ Montpellier, CNRS, INSERM, Montpellier, France

5 Department of Developmental and Cell Biology, University of California Irvine, CA, USA

6 Department of Mathematics, University of California Irvine, Irvine, CA, USA

7 Institute of Molecular Biosciences, Mahidol University, Nakhon Pathom, Thailand.

8 Centre Armand-Frappier Santé Biotechnologie, Institut National de la Recherche Scientifique, Laval, Québec, Canada

* Authors contributed equally.

# Authors contributed equally.

¶ Corresponding author: Julien.pompon@ird.fr

ABSTRACT

Cutaneous events determining transmission of mosquito-borne orthoflaviviruses remain largely uncharacterized. Here, we report single-cell RNA-sequencing of skin from immunocompetent mice exposed to West Nile virus-infected mosquitoes, capturing early response at a critical transmission bottleneck. Skin-resident fibroblasts, keratinocytes, and myeloid cells were exposed to infectious saliva. At the bite site, neutrophils and mast cells diminished, while lymphoid cells augmented. Cell-cell communication analysis showed that structural skin cells activate immune signaling targeting myeloid populations, which signal to lymphoid cells. Transcriptional profiling revealed cell subtype-specific responses integrating immune activation, skin repair and metabolic remodeling. Using *in vivo* gene silencing, we demonstrated that fibroblast-expressed LRRC15 (leucine rich repeat-containing 15) functions as a restriction factor, limiting viral replication in skin, viral dissemination to draining lymph nodes, and disease severity. Collectively, our transcriptomic-resolution and functional analyses provide cellular and molecular understanding of bite-initiated arboviral transmission, establishing skin-resident fibroblasts as frontline defender cells.

Key words: Arbovirus transmission, Mosquito bite-initiated skin infection, West Nile virus, Single-cell transcriptomics, Mosquito bite, Skin immunology, Dermal fibroblasts, LRRC15, Antiviral restriction factors, Cell-cell communication, Mouse model.

HIGHLIGHTS

* Single-cell RNA-sequencing captures early cutaneous response to West Nile virus-infected mosquito bites.

* Skin-resident fibroblasts, keratinocytes and myeloid cells are exposed to infectious mosquito saliva.

* Infectious bite induces rapid cellular remodeling and activates immune signaling networks from structural cells to myeloid and lymphoid populations.

* Bite-induced fibroblast-expressed LRRC15 restricts viral transmission and attenuates disease severity.

INTRODUCTION

Mosquito-borne orthoflaviviruses—including West Nile virus (WNV), dengue virus (DENV) and Zika virus (ZIKV)—cause recurrent outbreaks worldwide, infecting an estimated half a billion people each year and imposing considerable health and economic burden[1,2]. Existing vaccines remain limited and raise safety concerns, complicating both their design and clinical evaluation[3–6]. No antiviral drugs are licensed to-date and therapeutic approaches for acute infection are constrained by an extremely narrow treatment window[7,8]. These challenges underscore the urgent need for novel intervention strategies for mosquito-transmitted infectious diseases.

Bite-initiated skin infection is a critical vulnerability in viral transmission, representing a potential therapeutic target[9,10]. During probing, virus-laden mosquito saliva is injected into the skin, initiating viral transmission through a coordinated molecular and cellular response[11–13]. Saliva and bite-triggered mechanical injury induce local tissue inflammation and increase vascular permeability, which together promote recruitment of host neutrophils. These neutrophils release chemoattractants that then drive tissue infiltration for dendritic cells (DC), macrophages and monocytes[14–21]. These infiltrating myeloid cells—themselves being highly susceptible to orthoflavivirus infection—fulfill their defensive immune function as antigen-presenting cells while concurrently carrying viruses to draining lymph nodes (LNs), and as such, enable systemic dissemination and disease transmission[16,17,21–25]. Bite-induced skin edema further facilitates initial virus replication by restricting virus dispersion and maintaining saliva-delivered inoculum[11,17,19]. This sequence of events unfolds with remarkable speed: transcriptional up-regulation of neutrophil-attracting chemokines and neutrophil influx occurs within 4 hours post-bite, myeloid cell infiltration by 6th hour[16,19] and viral spread to LNs within 12-24 hours[11,25–27].

Consistently, excision of the bitten skin site at 4 hours or therapeutic activation of antiviral defenses before 5th hour post-bite abolishes transmission[21,28].

Structural cells of the skin also contribute to these early events. Major structural skin cells—keratinocytes in the epidermis and ectodermal appendages, as well as fibroblasts in the dermis[29]—are likely among the first cells to encounter infectious mosquito saliva and their permissiveness to multiple orthoflaviviruses may influence disease transmission[20,30–33]. Upon infection, structural cells activate innate immune responses[32,34–37], including interferon (IFN) pathways, which reduce viral replication[33]. Infected fibroblasts, moreover, promote DCs' viral resistance and T cell recruitment[31,38], highlighting the importance of cell-cell communication in the cutaneous response to infectious bites.

Despite these insights, prevailing mechanistic models of bite-initiated viral transmission rely largely on indirect and approximate experimental systems—such as virus incubation of skin explants or dissociated skin cells *in vitro,* artificial needle-based injection of viruses with or without saliva or with mosquito salivary gland extracts into immunodeficient mice, uninfected bites followed by viral inoculation or uninfected bite alone[25,39–41]. However, the well-documented impact of mosquito bite on viral transmission kinetics, tissue tropism, cutaneous cells' gene expression and disease severity[17,42,43] calls for the use of an *in vivo* transmission model to study the early events of transmission. Here, we applied single-cell RNA-sequencing (scRNA-seq) to skin exposed to infectious mosquito bites in an immunocompetent mouse model to characterize the early molecular and cellular responses to viral transmission. Our study delineated rapid reorganization of the cellular landscape of the skin, identified the specific cell types that first encounter infectious saliva, mapped cell-cell communication and defined cell type-specific transcriptomic responses.

Finally, we developed an *in vivo* cutaneous gene depletion approach to identify a fibroblast-mediated antiviral program that restricts viral transmission.

RESULTS

Single-cell characterization of mouse skin bitten by infectious mosquitoes

To conduct informative scRNA-seq evaluation of infectious mosquito-bitten mouse skin, we first characterized the *in vivo* bite-initiated transmission dynamics in wild-type (WT) mice. Multiple mosquitoes infected with WNV by intrathoracic inoculation—to standardize the inoculum—were allowed to bite immunocompetent WT mice (Fig. S1A). All mosquitoes had infected salivary glands (Fig. S1B,C) and their bites induced viremia (peaking at 4 days post-bite), clinical signs of infection, prominent weight loss and mortality in experimental mice (Fig. S1D-G; Dataset S1A,B), thereby validating efficient viral transmission. To define an optimal time point for the scRNA-seq assay, we next characterized viral infection kinetics in the bitten skin. We developed a method for precise identification of the bite site: individually caged mosquitoes (as described in[13]) (Fig. S2A,B) were placed on shaved mouse abdomen and access to the skin was further directed by applying tape perforated with four 2 mm-diameter openings (Fig. S2C,D). Visually identified bite sites were marked and collected from 10 minutes to 24 hours post-bite (Fig. S2E). Because the mosquito proboscis penetrates < 2 mm in any direction into mouse skin[13], we collected 2-mm-diameter skin biopsies and used them to quantify WNV genomic RNA (gRNA) (Fig. 1A). At 10 minutes post-bite, before virus amplification[44,45], ~10^4 copies of gRNA were expectorated into the skin. This gRNA level remained stable until 3 hours post-bite (hpb), then declined at 6-to-9 hpb—matching the time of viral genome replication onset[44,45]—before increasing to ~9.6 x 10^4 copies at 24 hpb, indicating virus

multiplication. To verify dissemination, WNV gRNA was quantified in draining LNs (Fig. 1B). Viral gRNA was detected as early as 10 minutes post-bite (geometric mean, 345 gRNA copies per LN), remained stable until 9 hpb, and then sharply increased to ~4.1 x 10^4 copies at 24 hpb, validating systemic infection. Based on these kinetics, we selected 6 hpb for cutaneous scRNA-seq analysis, a time point corresponding to the bottleneck phase characterized by transient reduction in cutaneous viral load and the absence of detectable viral expansion in draining LNs.

To perform scRNA-seq on skin at 6 hpb (Fig. 1C), we collected 2-mm biopsies centered on the bite sites in order to enrich for cells directly exposed to infectious saliva and processed tissues for single-cell isolation and capture. To minimize inter-sample variability and to reduce animal use, each mouse received between 3 and 5 bites, yielding multiple skin biopsies per individual. Multiple bites did not alter local cutaneous viral load at 24 hpb (Fig. S1H) but increased the viral inoculum reaching draining LNs (Fig. S1I). We optimized skin cell dissociation using enzymatic digestion combined with needle-assisted mechanical disruption to improve recovery of viable cells, including DCs and Langerhans cells (Fig. S3). Skin from non-bitten WT mice (hereafter referred to as resting skin) was identically processed and served as a control. After sequencing, genome mapping, quality controls and bioinformatic sample integration (Fig. S4), we obtained > 6,000 high quality sequenced cells per experimental condition (Fig. 1D).

Unsupervised clustering identified eight cell types (Fig. 1E), each defined by a distinct transcriptional signature (Fig. 1F; Dataset S2), including established cell type-specific marker genes (Fig. S5A-H). Fibroblasts were the predominant cell population (~62.5%), followed by keratinocytes (~15%) and immune cells of the myeloid (~9.4%) and lymphoid (~7.3%) lineages. Lymphatic (~3.1%) and vascular (~1.6%) endothelial

cells (EC), that delineate lymphatic and blood vessels, respectively, were also detected, along with vascular smooth muscle cells (SMC) (~0.5%), which surround larger blood vessels to regulate blood flow. A minor proportion of melanocytes was also observed (~0.4%). These cellular compositions were consistent with prior cutaneous scRNA-seq datasets[46].

To refine cell annotations, we subclustered the four major cell types based on subtype-enriched genes (Fig. S6; Dataset S3). Fibroblasts segregated into eight subtypes (Fig. 1G): CCL19^{+} fibroblasts (~46% of all fibroblasts), which promote tertiary lymphoid structures by recruiting lymphocytes and enhancing local adaptive immune response[47,48]; dermal white adipose tissue (dWAT) fibroblast cells (~28.2%), which reside beneath the dermis and contribute to wound healing, immune defenses and skin homeostasis[49]; Pi16^{+} fibroblasts (~7.3%), which form perivascular sheaths that regulates vascular stability, immune cell extravasation and stromal organization through extracellular matrix (ECM) production and expression of adhesion molecules and chemokines[50–53]; dermal sheath fibroblasts (~6.4%), which create a contractile niche layer around hair follicles, anchoring them within the skin and participating in dermal repair[54,55]; Crabp1^{+} fibroblasts (~4.3%), which modulate retinoic acid signaling, regulating ECM and dermal homeostasis[56,57]; telogen (~3.1%) and anagen (~2.5%) dermal papilla (DP) fibroblasts, which constitute the principal hair follicle signaling niche cells and reside at its base, with telogen DP cells maintaining follicle's quiescence, and anagen DP cells driving active hair growth[58]; and proliferating fibroblasts (~1.1%), which actively divide to support cutaneous tissue growth, repair and remodeling[59]. Epidermal and ectodermal appendage cells segregated into nine subtypes (Fig. 1H) listed in the order of decreasing abundance: germinative layer cells (~28.5% of all keratinocytes) [60], that reside at the base of growing hair follicles

where they actively divide, contributing to the steady-state hair growth[61]; suprabasal keratinocytes (~12.6%), which form upper layers of the epidermis where they differentiate to form water-tight barrier[61]; sebaceous gland cells (~11.4%), which produce lipid-rich secretome to lubricate epidermis and hairs, reinforce epidermal barrier and modulate local immune and antibacterial defenses[62]; hair follicle stem cells (HFSCs) (~8.7%), which reside in the so-called bulge region of the follicle, and critically sustain cyclical hair growth and contribute to epidermal repair after wounding[61]; upper hair follicle keratinocytes (~8.3%), which form a protective epithelium at the boundary with the epidermis[61]; cortex/cuticle cells (~8.1%) and medulla cells (~2.1%), which represent differentiated cell types of the hair shaft; basal keratinocytes (~14.8%), which form the deepest epidermal layer and maintain epidermal attachment[63]; and inner root sheath (IRS) keratinocytes (~6.6%), which form a protective sleeve around the growing hair shaft[64]. Among myeloid cells (Fig. 1I), we identified: macrophages (~34.4% of all myeloid cells); dendritic cells (~30.4%); mast cells (~15.7%); monocytes (~10.5%); Langerhans cells (~5.8%); and neutrophils (~3.2%). Among lymphoid cells (Fig. 1J), subclustering distinguished: T cells (~46% of all lymphoid cells), natural killer (NK) cells (~33.2%) and B cells (~20.1%). Altogether, these data establish a robust scRNA-seq framework to investigate mosquito bite–initiated viral infection in the skin at single-cell resolution.

Mosquito saliva interacts with multiple skin cell types and triggers transcriptional response in fibroblasts

As mosquito RNA is secreted into the saliva[65,66], we leveraged it as a molecular proxy to identify skin cell types that directly interact with infectious saliva

207 components. Non-polyadenylated viral reads could not be detected with the
208 scRNAseq technology. Upon data mapping, we aligned scRNA-seq reads against the
209 mosquito genome. Nearly 300 mosquito-derived reads were detected in bitten skin
210 (after quality controls), whereas none were found in resting control skin. Detected
211 mosquito reads mapped to six genes, two of which—*HISTONE H4* and an
212 uncharacterized locus (*LOC23687614*)—accounted for the large majority (Fig. 2A).
213 Mosquito RNA was detected in 3.9% of all sequenced mouse cells (Fig. 2B),
214 providing an estimate of the limited subset of skin cells directly exposed to mosquito
215 saliva, even with our narrow skin collection method. All annotated skin cell types,
216 except melanocytes, contained mosquito RNA; however, fibroblasts, vascular SMC
217 and keratinocytes exhibited the highest proportion of positive cells (~ 4%), with
218 fibroblasts representing the most exposed in absolute numbers (Fig. 2C). Moreover,
219 only fibroblasts, keratinocytes and myeloid cells contained more than one mosquito
220 read per cell (Fig. S7), further supporting their strong interaction with mosquito saliva.
221 Intriguingly, among fibroblasts, the distribution of mosquito RNA did not match
222 subtype abundance: proliferating (i.e., the least prevalent subtype) and dWAT
223 fibroblasts exhibited the highest frequencies of mosquito RNA positive cells, followed
224 by CCL19^{+} (i.e., the most prevalent subtype) and Crapb1^{+} fibroblasts (Fig. 2D). This
225 suggests preferential exposure or uptake by specific fibroblast subsets.

226 Next, we characterized transcriptional response to infectious mosquito saliva
227 by comparing gene expression patterns between mosquito RNA-positive and -
228 negative fibroblasts, identifying 20 significantly upregulated genes (Fig. 2E, Dataset
229 S4). Other cell types contained too few mosquito RNA-positive cells to support
230 statistically robust analyses. In fibroblasts, several enriched genes were associated
231 with skin repair and tissue remodeling: *DMKN,* known for promoting cutaneous

barrier formation[67]; *EFNB1,* an adhesion molecule with an established role in promoting angiogenesis[68]; and *DMPK,* a protein kinase that drives myoblast differentiation[69]. Three other differentially expressed genes (DEGs) promote cell motility: *MYLK* and *MYO18A* alter cytoskeleton[70,71], while *UCHL3* influences epithelial-mesenchymal transition[72]. Five additional DEGs are involved in general cellular homeostasis: *LVRN* is implicated in ECM remodeling[73]; *TPD52* and *RBP1* in promoting cell proliferation[74,75]; *CARMN*, a long non-coding RNA, in regulating cell differentiation[76]; and *VPS37B* in endosomal sorting through the ESCRT pathway[77]. Moreover, four other DEGs are related to metabolic pathways, inducing steroid biosynthesis (*DHCR24*[78] and *FDFT1*[79]) and energy-producing glycolysis (*ACSS2*[80] and *PFKFB3*[81]). Finally, four DEGs are associated with immune-related functions: *FXYD3* enhances IL-17A signalling, promoting cutaneous inflammation[82]; *H2-EB1* encodes an MHC class II protein that drives adaptive immune activation[83]; *DUSP22* modulates T cell activation through the JNK pathway[84]; and *STEAP4* responds to inflammation-induced oxidative stress[85]. Collectively, these scRNA-seq analyses provide the first single-cell-level identification of cutaneous cell types exposed to mosquito saliva and highlight fibroblasts, a structural cell type, as primary responders during the earliest stages of vector-host interactions.

Infectious bite drives rapid remodeling of the structural and immune cellular landscape

To characterize cutaneous cellular dynamics in response to infectious bites, we compared the cellular composition of bitten *vs.* resting skin in our scRNA-seq dataset via permutation testing. At the cell type level, we observed a reduction in melanocyte and keratinocyte populations, whereas vascular SMCs, lymphoid cells, vascular and

lymphatic ECs expanded following infectious bites (Fig. 3A-C). Among fibroblasts, telogen DP cells were markedly enriched upon infectious bite (Fig. 3D-F). Among keratinocytes and ectodermal appendage cells, populations of germinative layer, medulla, cortex and IRS strongly contracted, while sebaceous and suprabasal keratinocyte populations expanded (Fig. 3G-I). Among immune cells, abundance of mast cells and neutrophils was reduced (Fig. 3J-L), whereas B cells and NK cells were recruited to the bite site (Fig. 3M-O). Interestingly, population sizes of DCs, Langerhans cells, macrophages and monocytes remained largely unchanged at 6 hpb. Collectively, while hair follicle cell population differences might reflect natural hair cycle heterogeneity between animals, differences in non-hair cell types reveal rapid and extensive multicellular remodeling of the skin in response to an infectious bite, detectable as early as 6 hours post-exposure.

Infectious bite triggers cell-cell communication from structural to myeloid and lymphoid cells

To investigate how an infectious bite reshapes microenvironmental signaling in the skin, we inferred cell-cell communication (CCC) activity between cell subtypes from the scRNA-seq dataset using CellChat[86,87]. The CellChat database annotates ligands, receptors, and signaling agonists/antagonists across all known CCC pathways. First, we assessed global shifts in CCC of the skin by aggregating all ligand-receptor interactions significantly present in the data (Fig. 4A). This overview revealed that infectious bite enhanced communication between fibroblast subtypes, while reducing signaling from fibroblasts to keratinocytes and between keratinocyte subtypes. Among fibroblasts, Crabp1^{+} cells exhibited the strongest activation, both as signal senders and receivers. Among immune cells, communication across myeloid

subtypes was moderately increased. Next, we quantified the activity of individual CCC pathways. Of 56 pathways that were detected as active, 23 were upregulated and 10 downregulated by infectious bite (Fig. 4B). Notably, upregulated pathways were predominantly immune-related (17 out 23), whereas downregulated pathways were mostly associated with skin repair (7 out of 10).

Finally, we mapped activity of regulated pathways to specific cell subtypes (Fig. 4C, D) and detailed their contributions as either signal senders, receivers, mediators and/or influencers (Fig. S8). Focusing on immunity, we synthesized the upregulated communications (Fig. 4E), revealing overall immune CCC patterns. Fibroblasts activated eight CCC pathways toward keratinocytes and myeloid cells—particularly toward monocytes, mast cells and Langerhans cells. Crabp1^{+} and dWAT fibroblasts were the most active, inducing complement, CADM and FLT3 signaling toward myeloid cell subtypes, and SEM5 and CADM signaling toward most keratinocyte subtypes. Keratinocytes activated five CCC pathways directed toward DCs, neutrophils, mast cells and NK cells. Among keratinocytes, upper hair follicle keratinocytes were the most active, inducing CD200 signaling toward mast cells and DCs, and MHC-I signaling toward NK cells. Suprabasal keratinocytes induced LXA4 signaling with neutrophils, while most keratinocyte subtypes engaged in reciprocal SEMA5 signaling. From myeloid cells, nine pathways were activated. Monocytes were the dominant signal senders, triggering TGFβ and SIRP signaling toward Crabp1^{+} fibroblasts, and BST2 signaling toward mast cells and monocytes. Four pathways were directed toward lymphoid cells: mast cells induced SN signaling toward all lymphoid subtypes, Langerhans cells triggered ICOS signaling toward T cells, while neutrophils activated PD-L1 signaling toward B cells, and DCs induced PVR signaling toward NK cells. Neutrophils also communicated with mast cells

through CSF signaling. Among lymphoid cell populations, only NK cells induced one outgoing pathway, activating CD96 toward DCs. Taken together, these CellChat analyses demonstrate that infectious bite rapidly reprograms the cutaneous signaling network by dampening pathways involved in tissue repair, while amplifying immune-directed communication across stromal, epithelial and immune compartments. In particular, fibroblasts and keratinocytes activated multiple immune pathways targeting myeloid cells, which communicated with lymphoid populations.

Infectious bite induces mixed immunity, skin repair and metabolic transcriptional programs in a cell subtype-specific manner

To assess cell subtype-specific responses to infectious bite, we identified DEGs between infectious and resting condition within each cell subtype using a conservative fold-change threshold of ≥ 4, revealing 2,622 DEGs (Fig. 5A; Table S5). Keratinocytes and ectodermal appendages showed the most extensive transcriptional reprogramming (986 DEGs: 699 up, 287 down), with basal, cortex/cuticle, germinative layer, and IRS cells exhibiting the largest responses (>162 DEGs each), whereas HFSCs, medulla, sebaceous gland, and upper hair follicle cells had more modest responses (<66 DEGs each). Skin repair-associated genes were predominantly regulated, followed by immune-related genes, which accounted for more than 23.3% of DEGs in cortex/cuticle, germinative, HFSC, and IRS cells, with metabolic genes also being significantly modulated (Fig. S9A). Fibroblast subtypes featured fewer overall DEGs (753 DEGs: 289 up, 464 down) (Fig. 5A; Table S5), albeit Ccl19^{+}, Crabp1^{+}, dermal sheath, dWAT, and Pi16^{+} fibroblasts each had between 94 and 124 DEGs. Skin repair-associated genes were most regulated, followed by immune- and metabolic-related genes (Fig. S9A). Among myeloid cells

featuring 377 DEGs (202 up, 175 down) (Fig. 5A; Table S5), macrophages and DCs were the most responsive (>84 DEGs). Interestingly, skin repair-associated genes were also highly regulated across myeloid cell subtypes, while immune-related genes were most regulated in monocytes, neutrophils, and Langerhans cells. Metabolic genes were modulated across all myeloid cell subtypes (Fig. S9A). Among lymphoid cells, DEGs were predominantly downregulated (354 DEGs: 78 up, 276 down) and fairly homogeneous across NK, B, and T cells (125, 122, and 107 DEGs, respectively) (Fig. 5A; Table S5). Here too, skin repair-associated genes were predominant, followed by immune- and metabolic-related genes (Fig. S9A). Finally, lymphatic and vascular ECs and SMCs showed moderate responses (76, 54, and 22 DEGs, respectively) (Fig. 5A; Table S5), mainly involving skin repair, with minor immune- and metabolism-related regulation.

To refine the characterization of transcriptional remodeling across cell subtypes, we performed GO analyses on within-subtype upregulated DEGs using stringent thresholds (>10% DEGs; $p < 0.01$), presenting results in a decreasing order of cell abundance. Among fibroblasts (Fig. 5B), Ccl19^{+} fibroblasts showed robust activation of fatty-acid biosynthesis, accompanied by modulation of macrophage activation and induction of the pro-angiogenic program. dWAT fibroblasts predominantly upregulated immune-related processes, including several lymphoid-targeting chemoattractants and phagocytosis-related genes. Pi16^{+} and dermal sheath fibroblasts exhibited strong fatty-acid biosynthetic signatures and moderate chemotactic activity—directed toward T cells and macrophages in Pi16^{+} cells, or toward leukocytes more broadly in dermal sheath cells—and both contributed modestly to skin repair programs. In contrast, Crabp1^{+} fibroblasts strongly induced skin repair pathways, particularly those linked to angiogenesis and dermal

development, while moderately upregulating prostaglandin biosynthesis genes. Anagen DP fibroblasts preferentially activated T cell–related pathways, whereas telogen DP fibroblasts elicited a more modest neutrophil-attracting signature (Fig. S9B). Proliferating fibroblasts uniquely upregulated endothelial development pathway genes.

Among keratinocytes and ectodermal appendage cells (Fig. 5C), germinative cells markedly elicited granulocyte and neutrophil chemoattraction and antimicrobial humoral responses, while also contributing to ECM-driven and cell migratory processes associated with skin repair, but with minimal engagement of metabolic pathways. Basal keratinocytes predominantly activated skin-repair programs, including wound healing and skin development pathways, while minimally modulating immune or metabolic functions. Sebaceous glands displayed an immune-centric response focused on B-cell activation, together with the induction of tissue growth associated pathways. Cortex/cuticle cells almost exclusively upregulated skin repair programs, including several negative-regulatory processes. HFSCs and medulla cells each displayed only a single enriched biological process (Fig. S9C).

Among myeloid cells (Fig. 5D), macrophages showed modest activation of pro-angiogenic and fatty-acid pathways, without significant immune GO enrichment. DCs exhibited a mixed response, engaging fatty-acid metabolism, ECM-associated skin repair, and chemokine-related immune programs. Conversely, mast cells, monocytes, and neutrophils predominantly activated immune pathways—centered on chemokine responses in mast cells and monocytes, and on T cell-directed activity in neutrophils. Among lymphoid cell subtypes (Fig. 5E), NK cells lacked significant GO enrichment, whereas T cells did not upregulate classical immune-response pathways but, instead, prominently activated eicosanoid biosynthesis genes. B cells, in

contrast, activated chemotactic programs targeting DCs, neutrophils, and monocytes, and contributed moderately to skin development processes.

Finally, lymphatic ECs engaged a mix of immune, metabolic, and tissue repair responses; vascular ECs displayed modest immune-related signature; and vascular SMCs showed limited immune- and tissue repair-related activation (Fig. S9D-F). Together, these GO analyzes indicate that infectious mosquito bites trigger a multifaceted, cell subtype-specific transcriptional response integrating skin repair, immune activation, and metabolic adaptation across diverse tissue compartments, revealing specialized functions for distinct cell populations.

Fibroblast response to infectious bite reduces viral transmission

To determine how the above described cutaneous transcriptional responses contribute to viral transmission, we selected 14 immune-related DEGs identified in fibroblasts, myeloid, and lymphoid cells (Fig. 6A; Fig. S10A-C; Dataset S5) and assessed their regulation following *in vitro* exposure to virus, saliva (mimicking the bite), or both in lineage-matched human cell models: human foreskin fibroblasts (HFF1), monocytic U937 cells, and Jurkat T cells (Fig. 6B). Control experiments confirmed that the dye used for saliva collection[44] and saliva supplementation alone did not alter cell viability or infection rates (Fig. S10D,E). At 6 hours post-infection, six DEGs were modulated by virus, saliva, or their combination in a manner concordant with their *in vivo* regulation in mouse skin (Fig. 6C), whereas the remaining genes were unchanged or displayed inverse patterns (Fig. S10F). Next, we selected three representative genes for further functional interrogation: *LRRC15*, which was upregulated by infection in HFF1 cells, and *IFI30* and *HLA-DRB1* (the human ortholog of mouse *H2-EB1*), both of which were downregulated by infection in U937

cells (Fig. 6D). siRNA-mediated depletion of the three targets (Fig. S10G-I) and reduction of LRRC15 protein (Fig. S10J) showed that *HLA-DRB1* knockdown led to a moderate increase in viral replication (Fig. 6E), whereas *LRRC15* silencing triggered a markedly stronger enhancement (Fig. 6F), indicating that both genes possess antiviral activity, with LRRC15 serving as a potent restriction factor.

We developed an *in vivo* cutaneous siRNA-mediated silencing approach to investigate the effect of *LRRC15* in transmission (Fig. 6G). Forty-eight hours after siRNA injection, when cutaneous levels of *LRRC15* transcript (Fig. 6H) and protein (Fig. 6I,J) were reduced, mouse skin site was exposed to infectious bites. Local LRRC15 depletion enhanced viral load in both skin (Fig. 6K) and draining LNs (Fig. 6L) at 24 hpb. Furthermore, while RNAemia at 4 days post-bite confirmed transmission (Fig. S10K), *LRRC15* silencing exacerbated weight loss (Fig. 6M), disease severity (Fig. 6N; Dataset S1) and animal mortality (Fig. 6O). Collectively, these findings demonstrate that fibroblast-expressed *LRRC15* functions as a critical antiviral factor restraining early mosquito-borne infection and underscore the essential contribution of dermal fibroblast responses to arbovirus transmission.

Discussion

Initial cutaneous response to an infectious mosquito bite is a critical determinant of the arbovirus transmission success[41]. To capture the cellular and molecular architecture of this decisive early event in a relevant model, we developed scRNA-seq protocol on a small area of the skin bitten by WNV-infected mosquitoes in immunocompetent mice, precisely at the transmission bottleneck phase. Integrated bioinformatic analyses of skin cell composition, identification of mosquito saliva-exposed cells, inferred cell-cell communication networks, and cell type-specific

transcriptional programs provide an in-depth view of the earliest stage of arbovirus transmission. These data reveal distinct, subtype-specific cellular roles and highlight essential contribution of non-immune skin cells to infection establishment. Notably, using skin-localized gene depletion, we demonstrate that fibroblast-intrinsic responses are key determinants of transmission efficiency and downstream pathogenesis. Together, by leveraging newly-designed high-resolution and functional approaches, our study provides an integrated view of the multilevel, cross-cellular response to an infectious bite.

The orchestration of myeloid cell response in the skin is a critical driver of arbovirus transmission[41,88]. This response is first initiated by a rapid influx of neutrophils, detectable as early as 3 hours after an uninfectious bite in mice and 4 hours in humans, followed by a decline in neutrophil abundance by 5th hour post-bite in mice[17,19]. Consistent with this kinetic profile, we observed a reduced neutrophil population at 6 hours post-infectious bite, indicative of ongoing resolution of neutrophil-driven inflammation[89,90], further supported by the anti-inflammatory LXA4 signalling[91] toward neutrophils. Evidence for active inflammatory resolution was reinforced by the decreased abundance of mast cells, concomitant with the receipt of inhibitory CD200 signaling[92]. Rapid attenuation of bite-induced inflammation has similarly been described in human skin through the differentiation of anti-inflammatory M2 macrophages[19,93]. Despite these resolution-associated signatures, inflammation remained active at 6 hours post-infectious bite, as reflected by sustained TNF expression in neutrophils and IL33 and CCR5 in mast cells (Table S5), enrichment of multiple GO terms associated with chemoattraction, ongoing myeloid-promoting signaling through CSF[94] and complement pathway activation directed toward mast cells. We also observed a second wave of myeloid cell

recruitment[19,41], encompassing DC, macrophages and monocytes, although at low non-significant levels in our experimental conditions. All myeloid populations displayed a mixed transcriptional profile characterized by concurrent up- and down-regulation of cytokines, coexisting pro- and anti-inflammatory signaling pathways, and GO terms linked to leukocyte chemoattraction. Collectively, these findings delineate a tightly regulated cutaneous innate immune landscape following an infectious bite, in which inflammatory activation and resolution programs are simultaneously engaged. Our results detail with molecular resolution the dynamic and balanced nature of myeloid responses at early stages of bite-initiated transmission.

Within the lymphoid compartment, we observed a marked influx of NK cells, which contribute to early control of *Orthoflavivirus* infection[95,96]. As such recruitment is absent following uninfectious bites in human skin[19], it likely reflects virus-driven responses, consistent with mast cell-mediated NK cell recruitment to the skin upon viral sensing[97]. Infectious bite also increased B cell abundance, a cell type for which there is no data on its response to bite. Supporting the capacity for active cutaneous recruitment, B cells were recently shown to infiltrate skin upon bacterial infection[98] and we detected enhanced expression of DC-derived B cell chemoattractant CXCL13[99]. Despite an overall bias toward transcriptional repression, both NK and B cells were highly responsive to infectious bite, exhibiting bidirectional modulation of different inflammatory chemokines, interleukins, and immunoregulatory pathways, including inhibitory PVR signaling to NK cells[100] and PD-L1 signaling to B cells[101]. In contrast, T cells displayed stronger transcriptional overexpression and were targeted by activating signals such as ICOS, which promotes T cell proliferation[102,103] and SN, which induces phagocytic interactions[104]. Collectively, rapid recruitment and

activation of lymphoid cells at the bite site indicate their potential and previously underappreciated role in shaping early events that influence viral transmission.

Our untargeted approach details the contribution of non-immune structural cells, which have the capacity to mount an immune response[59,105], in actively shaping the cutaneous immune response to an infectious bite. All fibroblast and keratinocyte subtypes showed enrichment for inflammatory genes and chemoattraction pathways (Table S5), with dWAT fibroblasts and germinative keratinocytes exhibiting a particularly strong immune-associated transcriptional profile. Structural cells also displayed direct anti-viral features including defensins[106] in Ccl19^{+} and DP fibroblasts, and in basal, germinative, IRS, cortex/cuticle keratinocytes; cytotoxic mediators (granzymes and perforin) in dWAT and Pi16^{+} fibroblasts, and in germinative keratinocytes; pattern-recognition receptors (C-type lectins) in germinative keratinocytes; and multiple interferon-inducible genes (Table S5). CCC analyses suggest that fibroblasts—particularly dWAT cells—and keratinocytes—especially upper hair follicle populations—engage with myeloid cells, activating pathways linked to pathogen control (complement[107], ADGRB[108], CADM[109]), immune cell proliferation (FLT3[110], BST2[111]), recruitment (chemerin[112], SEMA5[113], L1CAM[114]), and regulation of inflammation (LXA4[91], CD200[92]). Together, these data indicate that structural skin cells adopt immune-active states following infectious bite, contributing to early innate defense and immune orchestration.

A major finding of our study is the *in vivo* identification of an anti-transmission response mediated by fibroblasts, revealing fibroblast-expressed LRRC15 as a potent restricting factor for WNV. Predominantly expressed in the skin[115,116], *LRRC15* encodes a membrane protein related to Toll-like receptors[115], a family of pattern-recognition receptors that initiate innate immune signaling[117,118]. Consistent with this

function, LRRC15 induces a robust antiviral program in fibroblasts and limits infection by SARS-CoV-2 and adenovirus[115,119], supporting a broad anti-viral function in line with our findings. Using localized depletion of LRRC15 in the skin, we demonstrate that LRRC15 restricts viral transmission and attenuates disease severity. A central unresolved question in vector-borne viral transmission concerns the identity of the initial target cells following exposure to infectious saliva. Our results indicate that productive infection of fibroblasts is required for transmission and, together with their pronounced exposure to bite-delivered virus, support the conclusion that fibroblasts constitute the initial cellular targets. Although virus is detectable in draining LNs as early as 10 minutes post-bite, consistent with rapid lymphatic dissemination, restricting local infection in fibroblasts markedly reduces LN seeding and disease outcome, establishing fibroblasts as critical regulators of early viral spread and transmission.

Limitations of the study

First, our analysis provides a snapshot of the skin response at 6 hpb, capturing early dynamics but not the full temporal trajectory of infection, immune activation, and tissue remodeling. Second, although mice provide a tractable and highly susceptible model for WNV, inter-species differences in skin architecture and immune composition may limit direct translation to humans. *In vitro* validation using human fibroblast and monocyte cell lines further lacks the multicellular complexity of intact skin, and siRNA approaches achieved only partial knockdown for some targets, leaving room for residual gene activity or off-target effects. Similarly, our study was conducted with one mosquito vector species and require further experimentation to expand our findings to other vectors. Finally, as our work centers on WNV, it remains

uncertain whether the identified fibroblast responses, including the restricting function of LRRC15, represent a generalizable mechanism across arboviruses.

Data and Code Availability

scRNA-seq data have been deposited at https://zenodo.org/records/17953412 and are publicly available as of the date of publication. Any additional information required to reanalyze the data reported in this paper is available from the Lead Contact upon request.

Acknowledgments

We thank all members of the Pompon's Laboratory at MIVEGEC, IRD, for their valuable suggestions and support. We are especially grateful to VectoPole team in Montpellier, particularly Bethsabée Scheid and Carole Ginibre, for providing mosquito eggs, and to Nathalie Barougier, Pascal Bautinaud and Drs. Sylvie Cornelie and Idris Mhaidi for their assistance with mouse management. We thank Dany Sevrac and the MGX-Montpellier GenomiX platfrom, part of the French National Infrastructure at the Montpellier Biocampus, for providing the Chromium system and technical support. We acknowledge the imaging facility MRI, member of the national infrastructure France-BioImaging (https://ror. org/01y7vt929) supported by the French National Research Agency (ANR-24-INBS-0005 FBI BIOGEN). Finally, we are grateful to Melanie Oakes and the Genomics Research and Technology Hub at the University of California, Irvine (UCI), USA, for sequencing support.

Funding

Support for this research came from fellowships from the Fondation pour la Recherche Médicale to H.M. (SPF202110013925) and to E.F.M. (ARF202309017577), Risques Infectieux et Vecteurs en Occitanie (RIVOC) and Key Initiatives MUSE Risques Infectieux et Vecteurs (KIM RIV) grants to H.M. and J.P., French Agence Nationale pour la Recherche (ANR-20-CE15-0006 to J.P. and ANR-21-CE15-0041 to S.N.), EU HORIZON-HLTH-2023-DISEASE-03-18 (#101137006) to J.P. and M.V.P., PHC Siam grant (#49487UJ) from the French Embassy in Thailand to J.P. and clinical fellowship from CIRM training grant (EDUC4-12822) to Y.L.

REFERENCES

1. Pierson, T.C., and Diamond, M.S. (2020). The continued threat of emerging flaviviruses. Nat. Microbiol. *5*, 796–812. https://doi.org/10.1038/s41564-020-0714-0.

2. Madere, F.S., Andrade da Silva, A.V., Okeze, E., Tilley, E., Grinev, A., Konduru, K., García, M., and Rios, M. (2025). Flavivirus infections and diagnostic challenges for dengue, West Nile and Zika Viruses. Npj Viruses *3*, 36. https://doi.org/10.1038/s44298-025-00114-z.

3. Santos-Peral, A., Luppa, F., Goresch, S., Nikolova, E., Zaucha, M., Lehmann, L., Dahlstroem, F., Karimzadeh, H., Thorn-Seshold, J., Winheim, E., et al. (2024). Prior flavivirus immunity skews the yellow fever vaccine response to cross-reactive antibodies with potential to enhance dengue virus infection. Nat. Commun. *15*, 1696. https://doi.org/10.1038/s41467-024-45806-x.

4. Halstead, S.B. (2021). Is Dengue Vaccine Protection Possible? Clin. Infect. Dis., ciab282. https://doi.org/10.1093/cid/ciab282.

5. Ferguson, N.M., Rodríguez-Barraquer, I., Dorigatti, I., Mier-y-Teran-Romero, L., Laydon, D.J., and Cummings, D.A.T. (2016). Benefits and risks of the Sanofi-Pasteur dengue vaccine: Modeling optimal deployment. Science *353*, 1033–1036. https://doi.org/10.1126/science.aaf9590.

6. WHO position paper on dengue vaccines, May 2024 https://www.who.int/publications/i/item/who-wer-9918-203-224.

7. Vegvari, C., Hadjichrysanthou, C., Cauët, E., Lawrence, E., Cori, A., Wolf, F. de, and Anderson, R.M. (2016). How Can Viral Dynamics Models Inform Endpoint Measures in Clinical Trials of Therapies for Acute Viral Infections? PLOS ONE *11*, e0158237. https://doi.org/10.1371/journal.pone.0158237.

8. Obi, J.O., Gutiérrez-Barbosa, H., Chua, J.V., and Deredge, D.J. (2021). Current Trends and Limitations in Dengue Antiviral Research. Trop. Med. Infect. Dis. *6*, 180. https://doi.org/10.3390/tropicalmed6040180.

9. Manning, J.E., Morens, D.M., Kamhawi, S., Valenzuela, J.G., and Memoli, M. (2018). Mosquito Saliva: The Hope for a Universal Arbovirus Vaccine? J. Infect. Dis. *218*, 7–15. https://doi.org/10.1093/infdis/jiy179.

10. Marín-López, A., Raduwan, H., Chen, T.-Y., Utrilla-Trigo, S., Wolfhard, D.P., and Fikrig, E. (2023). Mosquito Salivary Proteins and Arbovirus Infection: From Viral Enhancers to Potential Targets for Vaccines. Pathog. Basel Switz. *12*, 371. https://doi.org/10.3390/pathogens12030371.

11. Styer, L.M., Kent, K.A., Albright, R.G., Bennett, C.J., Kramer, L.D., and Bernard, K.A. (2007). Mosquitoes Inoculate High Doses of West Nile Virus as They Probe and Feed on Live Hosts. PLOS Pathog. *3*, e132. https://doi.org/10.1371/journal.ppat.0030132.

12. Choumet, V., Attout, T., Chartier, L., Khun, H., Sautereau, J., Robbe-Vincent, A., Brey, P., Huerre, M., and Bain, O. (2012). Visualizing Non Infectious and Infectious Anopheles gambiae Blood Feedings in Naive and Saliva-Immunized Mice. PLOS ONE *7*, e50464. https://doi.org/10.1371/journal.pone.0050464.

13. Wei Xiang, B.W., Saron, W.A.A., Stewart, J.C., Hain, A., Walvekar, V., Missé, D., Thomas, F., Kini, R.M., Roche, B., Claridge-Chang, A., et al. (2022). Dengue virus infection modifies mosquito blood-feeding behavior to increase transmission to the host. Proc. Natl. Acad. Sci. U. S. A. *119*, e2117589119. https://doi.org/10.1073/pnas.2117589119.

14. Lefteri, D.A., Bryden, S.R., Pingen, M., Terry, S., McCafferty, A., Beswick, E.F., Georgiev, G., Van der Laan, M., Mastrullo, V., Campagnolo, P., et al. (2022).

Mosquito saliva enhances virus infection through sialokinin-dependent vascular leakage. Proc. Natl. Acad. Sci. *119*, e2114309119. https://doi.org/10.1073/pnas.2114309119.

15. Hastings, A.K., Uraki, R., Gaitsch, H., Dhaliwal, K., Stanley, S., Sproch, H., Williamson, E., MacNeil, T., Marin-Lopez, A., Hwang, J., et al. (2019). Aedes aegypti NeSt1 Protein Enhances Zika Virus Pathogenesis by Activating Neutrophils. J. Virol. *93*, e00395-19. https://doi.org/10.1128/JVI.00395-19.

16. Wang, Z., Nie, K., Liang, Y., Niu, J., Yu, X., Zhang, O., Liu, L., Shi, X., Wang, Y., Feng, X., et al. (2024). A mosquito salivary protein-driven influx of myeloid cells facilitates flavivirus transmission. EMBO J. *43*, 1690–1721. https://doi.org/10.1038/s44318-024-00056-x.

17. Pingen, M., Bryden, S.R., Pondeville, E., Schnettler, E., Kohl, A., Merits, A., Fazakerley, J.K., Graham, G.J., and McKimmie, C.S. (2016). Host Inflammatory Response to Mosquito Bites Enhances the Severity of Arbovirus Infection. Immunity *44*, 1455–1469. https://doi.org/10.1016/j.immuni.2016.06.002.

18. Uraki, R., Hastings, A.K., Marin-Lopez, A., Sumida, T., Takahashi, T., Grover, J.R., Iwasaki, A., Hafler, D., Montgomery, R.R., and Fikrig, E. (2019). Aedes aegypti AgBR1 antibodies modulate early Zika virus infection of mice. Nat. Microbiol. *4*, 948–955. https://doi.org/10.1038/s41564-019-0385-x.

19. Guerrero, D., Vo, H.T.M., Lon, C., Bohl, J.A., Nhik, S., Chea, S., Man, S., Sreng, S., Pacheco, A.R., Ly, S., et al. (2022). Evaluation of cutaneous immune response in a controlled human in vivo model of mosquito bites. Nat. Commun. *13*, 7036. https://doi.org/10.1038/s41467-022-34534-9.

20. Duangkhae, P., Erdos, G., Ryman, K.D., Watkins, S.C., Falo, L.D., Marques, E.T.A., and Barratt-Boyes, S.M. (2018). Interplay between Keratinocytes and Myeloid

Cells Drives Dengue Virus Spread in Human Skin. J. Invest. Dermatol. *138*, 618–626. https://doi.org/10.1016/j.jid.2017.10.018.

21. Schmid, M.A., Glasner, D.R., Shah, S., Michlmayr, D., Kramer, L.D., and Harris, E. (2016). Mosquito Saliva Increases Endothelial Permeability in the Skin, Immune Cell Migration, and Dengue Pathogenesis during Antibody-Dependent Enhancement. PLoS Pathog. *12*, e1005676. https://doi.org/10.1371/journal.ppat.1005676.

22. Wu, S.-J.L., Grouard-Vogel, G., Sun, W., Mascola, J.R., Brachtel, E., Putvatana, R., Louder, M.K., Filgueira, L., Marovich, M.A., Wong, H.K., et al. (2000). Human skin Langerhans cells are targets of dengue virus infection. Nat. Med. *6*, 816–820. https://doi.org/10.1038/77553.

23. Cerny, D., Haniffa, M., Shin, A., Bigliardi, P., Tan, B.K., Lee, B., Poidinger, M., Tan, E.Y., Ginhoux, F., and Fink, K. (2014). Selective Susceptibility of Human Skin Antigen Presenting Cells to Productive Dengue Virus Infection. PLOS Pathog. *10*, e1004548. https://doi.org/10.1371/journal.ppat.1004548.

24. Martin, M.-F., Maarifi, G., Abiven, H., Seffals, M., Mouchet, N., Beck, C., Bodet, C., Lévèque, N., Arhel, N.J., Blanchet, F.P., et al. (2022). Usutu Virus escapes langerin-induced restriction to productively infect human Langerhans cells, unlike West Nile virus. Emerg. Microbes Infect. *11*, 761–774. https://doi.org/10.1080/22221751.2022.2045875.

25. Reynoso, G.V., Gordon, D.N., Kalia, A., Aguilar, C.C., Malo, C.S., Aleshnick, M., Dowd, K.A., Cherry, C.R., Shannon, J.P., Vrba, S.M., et al. (2023). Zika virus spreads through infection of lymph node-resident macrophages. Cell Rep. *42*. https://doi.org/10.1016/j.celrep.2023.112126.

26. Kyle, J.L., Beatty, P.R., and Harris, E. (2007). Dengue Virus Infects Macrophages and Dendritic Cells in a Mouse Model of Infection. J. Infect. Dis. *195*, 1808–1817. https://doi.org/10.1086/518007.

27. Lim, P.-Y., Behr, M.J., Chadwick, C.M., Shi, P.-Y., and Bernard, K.A. (2011). Keratinocytes Are Cell Targets of West Nile Virus In Vivo. J. Virol. *85*, 5197–5201. https://doi.org/10.1128/jvi.02692-10.

28. Bryden, S.R., Pingen, M., Lefteri, D.A., Miltenburg, J., Delang, L., Jacobs, S., Abdelnabi, R., Neyts, J., Pondeville, E., Major, J., et al. (2020). Pan-viral protection against arboviruses by activating skin macrophages at the inoculation site. Sci. Transl. Med. *12*. https://doi.org/10.1126/scitranslmed.aax2421.

29. Mirzayev, M. (2025). ANATOMY OF THE SKIN: STRUCTURE AND FUNCTIONS OF THE EPIDERMIS AND DERMIS. Int. J. Med. Sci. *1*, 302–306.

30. Arnold, S.J., Osvath, S.R., Hall, R.A., King, N.J.C., and Sedger, L.M. (2004). Regulation of antigen processing and presentation molecules in West Nile virus-infected human skin fibroblasts. Virology *324*, 286–296. https://doi.org/10.1016/j.virol.2004.03.036.

31. Montes-Gómez, A.E., García-Cordero, J., Marcial-Juárez, E., Shrivastava, G., Visoso-Carvajal, G., Juárez-Delgado, F.J., Flores-Romo, L., Sanchez-Torres, M.C., Santos-Argumedo, L., Bustos-Arriaga, J., et al. (2020). Crosstalk Between Dermal Fibroblasts and Dendritic Cells During Dengue Virus Infection. Front. Immunol. *11*, 538240. https://doi.org/10.3389/fimmu.2020.538240.

32. Kim, J.-A., Seong, R.-K., Son, S.W., and Shin, O.S. (2019). Insights into ZIKV-Mediated Innate Immune Responses in Human Dermal Fibroblasts and Epidermal Keratinocytes. J. Invest. Dermatol. *139*, 391–399. https://doi.org/10.1016/j.jid.2018.07.038.

33. Hoover, L.I., and Fredericksen, B.L. (2014). IFN-Dependent and -Independent Reduction in West Nile Virus Infectivity in Human Dermal Fibroblasts. Viruses *6*, 1424–1441. https://doi.org/10.3390/v6031424.

34. Hamel, R., Dejarnac, O., Wichit, S., Ekchariyawat, P., Neyret, A., Luplertlop, N., Perera-Lecoin, M., Surasombatpattana, P., Talignani, L., Thomas, F., et al. (2015). Biology of Zika Virus Infection in Human Skin Cells. J. Virol. *89*, 8880–8896. https://doi.org/10.1128/jvi.00354-15.

35. Garcia, M., Alout, H., Diop, F., Damour, A., Bengue, M., Weill, M., Missé, D., Lévêque, N., and Bodet, C. (2018). Innate Immune Response of Primary Human Keratinocytes to West Nile Virus Infection and Its Modulation by Mosquito Saliva. Front. Cell. Infect. Microbiol. *8*. https://doi.org/10.3389/fcimb.2018.00387.

36. Bustos-Arriaga, J., García-Machorro, J., León-Juárez, M., García-Cordero, J., Santos-Argumedo, L., Flores-Romo, L., Méndez-Cruz, A.R., Juárez-Delgado, F.J., and Cedillo-Barrón, L. (2011). Activation of the Innate Immune Response against DENV in Normal Non-Transformed Human Fibroblasts. PLoS Negl. Trop. Dis. *5*. https://doi.org/10.1371/journal.pntd.0001420.

37. López-González, M., Meza-Sánchez, D., García-Cordero, J., Bustos-Arriaga, J., Vélez-Del Valle, C., Marsch-Moreno, M., Castro-Jiménez, T., Flores-Romo, L., Santos-Argumedo, L., Gutiérrez-Castañeda, B., et al. (2018). Human keratinocyte cultures (HaCaT) can be infected by DENV, triggering innate immune responses that include IFNλ and LL37. Immunobiology *223*, 608–617. https://doi.org/10.1016/j.imbio.2018.07.006.

38. Bustos-Arriaga, J., Mita-Mendoza, N.K., Lopez-Gonzalez, M., García-Cordero, J., Juárez-Delgado, F.J., Gromowski, G.D., Méndez-Cruz, R.A., Fairhurst, R.M., Whitehead, S.S., and Cedillo-Barrón, L. (2016). Soluble mediators produced by the

crosstalk between microvascular endothelial cells and dengue-infected primary dermal fibroblasts inhibit dengue virus replication and increase leukocyte transmigration. Immunol. Res. *64*, 392–403. https://doi.org/10.1007/s12026-015-8675-8.

39. Martí, M.M., Castanha, P.M.S., and Barratt-Boyes, S.M. (2024). The Dynamic Relationship between Dengue Virus and the Human Cutaneous Innate Immune Response. Viruses *16*, 727. https://doi.org/10.3390/v16050727.

40. Garcia, M., Wehbe, M., Lévêque, N., and Bodet, C. (2017). Skin innate immune response to flaviviral infection. Eur. Cytokine Netw. *28*, 41–51. https://doi.org/10.1684/ecn.2017.0394.

41. Pingen, M., Schmid, M.A., Harris, E., and McKimmie, C.S. (2017). Mosquito Biting Modulates Skin Response to Virus Infection. Trends Parasitol. *33*, 645–657. https://doi.org/10.1016/j.pt.2017.04.003.

42. Dudley, D.M., Newman, C.M., Lalli, J., Stewart, L.M., Koenig, M.R., Weiler, A.M., Semler, M.R., Barry, G.L., Zarbock, K.R., Mohns, M.S., et al. (2017). Infection via mosquito bite alters Zika virus tissue tropism and replication kinetics in rhesus macaques. Nat. Commun. *8*, 2096. https://doi.org/10.1038/s41467-017-02222-8.

43. Cox, J., Mota, J., Sukupolvi-Petty, S., Diamond, M.S., and Rico-Hesse, R. (2012). Mosquito Bite Delivery of Dengue Virus Enhances Immunogenicity and Pathogenesis in Humanized Mice. J. Virol. *86*, 7637–7649. https://doi.org/10.1128/JVI.00534-12.

44. Medkour, H., Pruvost, L., Miot, E.F., Gong, X., Vaissayre, V., Tavadia, M., Boutinaud, P., Revel, J., Hitakarun, A., Sornjai, W., et al. (2025). Sphingomyelins in mosquito saliva reconfigure skin lipidome to promote viral protein levels and enhance

transmission of flaviviruses. Cell Metab. *0*. https://doi.org/10.1016/j.cmet.2025.05.015.

45. Barrows, N.J., Campos, R.K., Liao, K.-C., Prasanth, K.R., Soto-Acosta, R., Yeh, S.-C., Schott-Lerner, G., Pompon, J., Sessions, O.M., Bradrick, S.S., et al. (2018). Biochemistry and Molecular Biology of Flaviviruses. Chem. Rev. *118*, 4448–4482. https://doi.org/10.1021/acs.chemrev.7b00719.

46. Almet, A.A., Liu, Y., Nie, Q., and Plikus, M.V. (2025). Integrated Single-Cell Analysis Reveals Spatially and Temporally Dynamic Heterogeneity in Fibroblast States during Wound Healing. J. Invest. Dermatol. *145*, 645-659.e25. https://doi.org/10.1016/j.jid.2024.06.1281.

47. Zhang, Y., Liu, G., Zeng, Q., Wu, W., Lei, K., Zhang, C., Tang, M., Zhang, Y., Xiang, X., Tan, L., et al. (2024). CCL19-producing fibroblasts promote tertiary lymphoid structure formation enhancing anti-tumor IgG response in colorectal cancer liver metastasis. Cancer Cell *42*, 1370-1385.e9. https://doi.org/10.1016/j.ccell.2024.07.006.

48. Onder, L., Papadopoulou, C., Lütge, A., Cheng, H.-W., Lütge, M., Perez-Shibayama, C., Gil-Cruz, C., De Martin, A., Kurz, L., Cadosch, N., et al. (2025). Fibroblastic reticular cells generate protective intratumoral T cell environments in lung cancer. Cell *188*, 430-446.e20. https://doi.org/10.1016/j.cell.2024.10.042.

49. Li, Y., Long, J., Zhang, Z., and Yin, W. (2024). Insights into the unique roles of dermal white adipose tissue (dWAT) in wound healing. Front. Physiol. *15*, 1346612. https://doi.org/10.3389/fphys.2024.1346612.

50. Buechler, M.B., Pradhan, R.N., Krishnamurty, A.T., Cox, C., Calviello, A.K., Wang, A.W., Yang, Y.A., Tam, L., Caothien, R., Roose-Girma, M., et al. (2021).

Cross-tissue organization of the fibroblast lineage. Nature *593*, 575–579. https://doi.org/10.1038/s41586-021-03549-5.

51. Garrity, R., Arora, N., Haque, M.A., Weis, D., Trinh, R.T., Neerukonda, S.V., Kumari, S., Cortez, I., Ubogu, E.E., Mahalingam, R., et al. (2023). Fibroblast-derived PI16 sustains inflammatory pain via regulation of CD206+ myeloid cells. Brain. Behav. Immun. *112*, 220–234. https://doi.org/10.1016/j.bbi.2023.06.011.

52. Garrity, R., Haque, A., Kavelaars, A., Heijnen, C., and Shepherd, A. (2024). Fibroblast-derived PI16 Drives the Physiological Process of Immune Cell Recruitment and Activation During Inflammatory Response. J. Pain *25*, 13. https://doi.org/10.1016/j.jpain.2024.01.067.

53. McCartney, E.E., Chung, Y., and Buechler, M.B. (2024). Life of Pi: Exploring functions of Pi16+ fibroblasts. F1000Research *13*, 126. https://doi.org/10.12688/f1000research.143511.2.

54. Rahmani, W., Abbasi, S., Hagner, A., Raharjo, E., Kumar, R., Hotta, A., Magness, S., Metzger, D., and Biernaskie, J. (2014). Hair follicle dermal stem cells regenerate the dermal sheath, repopulate the dermal papilla, and modulate hair type. Dev. Cell *31*, 543–558. https://doi.org/10.1016/j.devcel.2014.10.022.

55. Joost, S., Zeisel, A., Jacob, T., Sun, X., La Manno, G., Lönnerberg, P., Linnarsson, S., and Kasper, M. (2016). Single-Cell Transcriptomics Reveals that Differentiation and Spatial Signatures Shape Epidermal and Hair Follicle Heterogeneity. Cell Syst. *3*, 221-237.e9. https://doi.org/10.1016/j.cels.2016.08.010.

56. Guerrero-Juarez, C.F., Dedhia, P.H., Jin, S., Ruiz-Vega, R., Ma, D., Liu, Y., Yamaga, K., Shestova, O., Gay, D.L., Yang, Z., et al. (2019). Single-cell analysis reveals fibroblast heterogeneity and myeloid-derived adipocyte progenitors in murine skin wounds. Nat. Commun. *10*, 650. https://doi.org/10.1038/s41467-018-08247-x.

57. Philippeos, C., Telerman, S.B., Oulès, B., Pisco, A.O., Shaw, T.J., Elgueta, R., Lombardi, G., Driskell, R.R., Soldin, M., Lynch, M.D., et al. (2018). Spatial and Single-Cell Transcriptional Profiling Identifies Functionally Distinct Human Dermal Fibroblast Subpopulations. J. Invest. Dermatol. *138*, 811–825. https://doi.org/10.1016/j.jid.2018.01.016.

58. Avigad Laron, E., Aamar, E., and Enshell-Seijffers, D. (2018). The Mesenchymal Niche of the Hair Follicle Induces Regeneration by Releasing Primed Progenitors from Inhibitory Effects of Quiescent Stem Cells. Cell Rep. *24*, 909-921.e3. https://doi.org/10.1016/j.celrep.2018.06.084.

59. Plikus, M.V., Wang, X., Sinha, S., Forte, E., Thompson, S.M., Herzog, E.L., Driskell, R.R., Rosenthal, N., Biernaskie, J., and Horsley, V. (2021). Fibroblasts: Origins, definitions, and functions in health and disease. Cell *184*, 3852–3872. https://doi.org/10.1016/j.cell.2021.06.024.

60. Joost, S., Annusver, K., Jacob, T., Sun, X., Dalessandri, T., Sivan, U., Sequeira, I., Sandberg, R., and Kasper, M. (2020). The Molecular Anatomy of Mouse Skin during Hair Growth and Rest. Cell Stem Cell *26*, 441-457.e7. https://doi.org/10.1016/j.stem.2020.01.012.

61. Blanpain, C., and Fuchs, E. (2009). Epidermal homeostasis: a balancing act of stem cells in the skin. Nat. Rev. Mol. Cell Biol. *10*, 207–217. https://doi.org/10.1038/nrm2636.

62. Zouboulis, C.C., Picardo, M., Ju, Q., Kurokawa, I., Törőcsik, D., Bíró, T., and Schneider, M.R. (2016). Beyond acne: Current aspects of sebaceous gland biology and function. Rev. Endocr. Metab. Disord. *17*, 319–334. https://doi.org/10.1007/s11154-016-9389-5.

63. Watt, F.M. (2014). Mammalian skin cell biology: at the interface between laboratory and clinic. Science *346*, 937–940. https://doi.org/10.1126/science.1253734.

64. Rogers, G.E. (2004). Hair follicle differentiation and regulation. Int. J. Dev. Biol. *48*, 163–170.

65. Maharaj, P.D., Widen, S.G., Huang, J., Wood, T.G., and Thangamani, S. (2015). Discovery of Mosquito Saliva MicroRNAs during CHIKV Infection. PLoS Negl. Trop. Dis. *9*. https://doi.org/10.1371/journal.pntd.0003386.

66. Fiorillo, C., Yen, P.-S., Colantoni, A., Mariconti, M., Azevedo, N., Lombardo, F., Failloux, A.-B., and Arcà, B. (2022). MicroRNAs and other small RNAs in Aedes aegypti saliva and salivary glands following chikungunya virus infection. Sci. Rep. *12*, 9536. https://doi.org/10.1038/s41598-022-13780-3.

67. Leclerc, E.A., Huchenq, A., Kezic, S., Serre, G., and Jonca, N. (2014). Mice deficient for the epidermal dermokine β and γ isoforms display transient cornification defects. J. Cell Sci. *127*, 2862–2872. https://doi.org/10.1242/jcs.144808.

68. Wang, H.U., Chen, Z.F., and Anderson, D.J. (1998). Molecular distinction and angiogenic interaction between embryonic arteries and veins revealed by ephrin-B2 and its receptor Eph-B4. Cell *93*, 741–753. https://doi.org/10.1016/s0092-8674(00)81436-1.

69. Elkins, J.M., Amos, A., Niesen, F.H., Pike, A.C.W., Fedorov, O., and Knapp, S. (2009). Structure of dystrophia myotonica protein kinase. Protein Sci. Publ. Protein Soc. *18*, 782–791. https://doi.org/10.1002/pro.82.

70. Cao, J.-M., Cheng, X.-N., Li, S.-Q., Heller, S., Xu, Z.-G., and Shi, D.-L. (2016). Identification of novel MYO18A interaction partners required for myoblast adhesion and muscle integrity. Sci. Rep. *6*, 36768. https://doi.org/10.1038/srep36768.

71. Lin, J., He, Y., Chen, L., Chen, X., Zang, S., and Lin, W. (2018). MYLK promotes hepatocellular carcinoma progression through regulating cytoskeleton to enhance epithelial-mesenchymal transition. Clin. Exp. Med. *18*, 523–533. https://doi.org/10.1007/s10238-018-0509-2.

72. Yang, Z., Wei, W., Nie, D., Zhang, M., and Chen, Q. (2025). UCHL3 regulates snail stability and promotes epithelial–mesenchymal transition in ovarian cancer. Cytotechnology *77*, 152. https://doi.org/10.1007/s10616-025-00811-w.

73. Feng, X., Wei, Z., Zhang, S., Zhou, J., Wu, J., Luan, B., Du, Y., and Zhao, H. (2021). Overexpression of LVRN impedes the invasion of trophoblasts by inhibiting epithelial-mesenchymal transition. Acta Biochim. Biophys. Sin. *53*, 249–257. https://doi.org/10.1093/abbs/gmaa167.

74. Zhang, S., Geng, Z., Sun, J., Chen, N., Liu, M., Wang, Y., Gu, X., and Pei, B. (2025). TPD52 promotes the proliferation and metastasis of gastric cancer cells. BMC Gastroenterol. *25*, 690. https://doi.org/10.1186/s12876-025-04295-y.

75. Yu, J., Perri, M., Jones, J.W., Pierzchalski, K., Ceaicovscaia, N., Cione, E., and Kane, M.A. (2022). Altered RBP1 Gene Expression Impacts Epithelial Cell Retinoic Acid, Proliferation, and Microenvironment. Cells *11*, 792. https://doi.org/10.3390/cells11050792.

76. Li, H., Sun, C., Luo, B., Zhan, C., Li, W., Deng, L., Kang, K., and Gou, D. (2024). Exploring the Spectrum of Long Non-Coding RNA CARMN in Physiological and Pathological Contexts. Biomolecules *14*, 954. https://doi.org/10.3390/biom14080954.

77. Bache, K.G., Slagsvold, T., Cabezas, A., Rosendal, K.R., Raiborg, C., and Stenmark, H. (2004). The growth-regulatory protein HCRP1/hVps37A is a subunit of

mammalian ESCRT-I and mediates receptor down-regulation. Mol. Biol. Cell *15*, 4337–4346. https://doi.org/10.1091/mbc.e04-03-0250.

78. Cheng, L., Xu, Y., Li, Z., Sun, D., Xu, Y., He, J., Chen, Y., and Yao, Q. (2025). DHCR24 overexpression is involved in lipid metabolic reprogramming to drive cervical cancer malignant progression and is associated with immune microenvironment. BMC Cancer *25*, 1291. https://doi.org/10.1186/s12885-025-14663-2.

79. Cai, D., Zhong, G.-C., Dai, X., Zhao, Z., Chen, M., Hu, J., Wu, Z., Cheng, L., Li, S., and Gong, J. (2025). Targeting FDFT1 Reduces Cholesterol and Bile Acid Production and Delays Hepatocellular Carcinoma Progression Through the HNF4A/ALDOB/AKT1 Axis. Adv. Sci. Weinh. Baden-Wurtt. Ger. *12*, e2411719. https://doi.org/10.1002/advs.202411719.

80. El-Kurjieh, A., Al-Arab, R., Hachem, Q.A., Ibrahim, J.-N., and Kobeissy, P.H. (2025). ACSS2 and metabolic diseases: from lipid metabolism to therapeutic target. Lipids Health Dis. *24*, 74. https://doi.org/10.1186/s12944-025-02491-z.

81. Houddane, A., Bultot, L., Novellasdemunt, L., Johanns, M., Gueuning, M.-A., Vertommen, D., Coulie, P.G., Bartrons, R., Hue, L., and Rider, M.H. (2017). Role of Akt/PKB and PFKFB isoenzymes in the control of glycolysis, cell proliferation and protein synthesis in mitogen-stimulated thymocytes. Cell. Signal. *34*, 23–37. https://doi.org/10.1016/j.cellsig.2017.02.019.

82. Yang, W., He, R., Qu, H., Lian, W., Xue, Y., Wang, T., Lin, W., Zhu, P., Xia, M., Lai, L., et al. (2023). FXYD3 enhances IL-17A signaling to promote psoriasis by competitively binding TRAF3 in keratinocytes. Cell. Mol. Immunol. *20*, 292–304. https://doi.org/10.1038/s41423-023-00973-7.

83. Charles A Janeway, J., Travers, P., Walport, M., and Shlomchik, M.J. (2001). The major histocompatibility complex and its functions. In Immunobiology: The Immune System in Health and Disease. 5th edition (Garland Science).

84. Li, J.-P., Fu, Y.-N., Chen, Y.-R., and Tan, T.-H. (2010). JNK Pathway-associated Phosphatase Dephosphorylates Focal Adhesion Kinase and Suppresses Cell Migration. J. Biol. Chem. *285*, 5472–5478. https://doi.org/10.1074/jbc.M109.060186.

85. Xue, X., Bredell, B.X., Anderson, E.R., Martin, A., Mays, C., Nagao-Kitamoto, H., Huang, S., Győrffy, B., Greenson, J.K., Hardiman, K., et al. (2017). Quantitative proteomics identifies STEAP4 as a critical regulator of mitochondrial dysfunction linking inflammation and colon cancer. Proc. Natl. Acad. Sci. U. S. A. *114*, E9608–E9617. https://doi.org/10.1073/pnas.1712946114.

86. Jin, S., Guerrero-Juarez, C.F., Zhang, L., Chang, I., Ramos, R., Kuan, C.-H., Myung, P., Plikus, M.V., and Nie, Q. (2021). Inference and analysis of cell-cell communication using CellChat. Nat. Commun. *12*, 1088. https://doi.org/10.1038/s41467-021-21246-9.

87. Jin, S., Plikus, M.V., and Nie, Q. (2025). CellChat for systematic analysis of cell-cell communication from single-cell transcriptomics. Nat. Protoc. *20*, 180–219. https://doi.org/10.1038/s41596-024-01045-4.

88. Yu, X., Zhu, Y., Yin, G., Wang, Y., Shi, X., and Cheng, G. (2024). Exploiting hosts and vectors: viral strategies for facilitating transmission. EMBO Rep. *25*, 3187–3201. https://doi.org/10.1038/s44319-024-00214-6.

89. Kolaczkowska, E., and Kubes, P. (2013). Neutrophil recruitment and function in health and inflammation. Nat. Rev. Immunol. *13*, 159–175. https://doi.org/10.1038/nri3399.

90. Greenlee-Wacker, M.C. (2016). Clearance of apoptotic neutrophils and resolution of inflammation. Immunol. Rev. *273*, 357–370. https://doi.org/10.1111/imr.12453.

91. Suchitha, G.P., Devasahayam Arokia Balaya, R., Prasad, T.S.K., and Dagamajalu, S. (2024). A signaling network map of Lipoxin (LXA4): an anti-inflammatory molecule. Inflamm. Res. Off. J. Eur. Histamine Res. Soc. Al *73*, 1099–1106. https://doi.org/10.1007/s00011-024-01885-6.

92. Vaine, C.A., and Soberman, R.J. (2014). The CD200-CD200R1 inhibitory signaling pathway: immune regulation and host-pathogen interactions. Adv. Immunol. *121*, 191–211. https://doi.org/10.1016/B978-0-12-800100-4.00005-2.

93. Yunna, C., Mengru, H., Lei, W., and Weidong, C. (2020). Macrophage M1/M2 polarization. Eur. J. Pharmacol. *877*, 173090. https://doi.org/10.1016/j.ejphar.2020.173090.

94. Hamilton, J.A., and Achuthan, A. (2013). Colony stimulating factors and myeloid cell biology in health and disease. Trends Immunol. *34*, 81–89. https://doi.org/10.1016/j.it.2012.08.006.

95. Costa, V.V., Ye, W., Chen, Q., Teixeira, M.M., Preiser, P., Ooi, E.E., and Chen, J. (2017). Dengue Virus-Infected Dendritic Cells, but Not Monocytes, Activate Natural Killer Cells through a Contact-Dependent Mechanism Involving Adhesion Molecules. mBio *8*, e00741-17. https://doi.org/10.1128/mBio.00741-17.

96. Maucourant, C., Petitdemange, C., Yssel, H., and Vieillard, V. (2019). Control of Acute Arboviral Infection by Natural Killer Cells. Viruses *11*, 131. https://doi.org/10.3390/v11020131.

97. St John, A.L., Rathore, A.P.S., Yap, H., Ng, M.-L., Metcalfe, D.D., Vasudevan, S.G., and Abraham, S.N. (2011). Immune surveillance by mast cells during dengue

infection promotes natural killer (NK) and NKT-cell recruitment and viral clearance. Proc. Natl. Acad. Sci. U. S. A. *108*, 9190–9195. https://doi.org/10.1073/pnas.1105079108.

98. Gribonika, I., Band, V.I., Chi, L., Perez-Chaparro, P.J., Link, V.M., Ansaldo, E., Oguz, C., Bousbaine, D., Fischbach, M.A., and Belkaid, Y. (2025). Skin autonomous antibody production regulates host-microbiota interactions. Nature *638*, 1043–1053. https://doi.org/10.1038/s41586-024-08376-y.

99. Shen, P., and Fillatreau, S. (2015). Antibody-independent functions of B cells: a focus on cytokines. Nat. Rev. Immunol. *15*, 441–451. https://doi.org/10.1038/nri3857.

100. Wu, B., Zhong, C., Lang, Q., Liang, Z., Zhang, Y., Zhao, X., Yu, Y., Zhang, H., Xu, F., and Tian, Y. (2021). Poliovirus receptor (PVR)-like protein cosignaling network: new opportunities for cancer immunotherapy. J. Exp. Clin. Cancer Res. CR *40*, 267. https://doi.org/10.1186/s13046-021-02068-5.

101. Ai, L., Xu, A., and Xu, J. (2020). Roles of PD-1/PD-L1 Pathway: Signaling, Cancer, and Beyond. Adv. Exp. Med. Biol. *1248*, 33–59. https://doi.org/10.1007/978-981-15-3266-5_3.

102. Hutloff, A., Dittrich, A.M., Beier, K.C., Eljaschewitsch, B., Kraft, R., Anagnostopoulos, I., and Kroczek, R.A. (1999). ICOS is an inducible T-cell co-stimulator structurally and functionally related to CD28. Nature *397*, 263–266. https://doi.org/10.1038/16717.

103. Yoshinaga, S.K., Whoriskey, J.S., Khare, S.D., Sarmiento, U., Guo, J., Horan, T., Shih, G., Zhang, M., Coccia, M.A., Kohno, T., et al. (1999). T-cell co-stimulation through B7RP-1 and ICOS. Nature *402*, 827–832. https://doi.org/10.1038/45582.

104. Klaas, M., Dubock, S., Ferguson, D.J.P., and Crocker, P.R. (2023). Sialoadhesin (CD169/Siglec-1) is an extended molecule that escapes inhibitory cis-interactions and synergizes with other macrophage receptors to promote phagocytosis. Glycoconj. J. *40*, 213–223. https://doi.org/10.1007/s10719-022-10097-1.

105. Simmons, J., and Gallo, R.L. (2024). The Central Roles of Keratinocytes in Coordinating Skin Immunity. J. Invest. Dermatol. *144*, 2377–2398. https://doi.org/10.1016/j.jid.2024.06.1280.

106. Ding, J., Chou, Y.-Y., and Chang, T.L. (2009). Defensins in viral infections. J. Innate Immun. *1*, 413–420. https://doi.org/10.1159/000226256.

107. Charles A Janeway, J., Travers, P., Walport, M., and Shlomchik, M.J. (2001). The complement system and innate immunity. In Immunobiology: The Immune System in Health and Disease. 5th edition (Garland Science).

108. Tseng, W.-Y., Stacey, M., and Lin, H.-H. (2023). Role of Adhesion G Protein-Coupled Receptors in Immune Dysfunction and Disorder. Int. J. Mol. Sci. *24*, 5499. https://doi.org/10.3390/ijms24065499.

109. Darlington, K.C., Shumway, A.J., Sona, C., Khaled, Z., Steinbach, E.C., Kikuchi, Y., Fan, S., Gartner, V., Clough, K.M., Nishiyama, N.C., et al. (2026). Myeloid Cell Adhesion Molecule 1 (CADM1) Promotes Proinflammatory Signaling in Human Inflammatory Bowel Diseases. Cell. Mol. Gastroenterol. Hepatol. *20*, 101618. https://doi.org/10.1016/j.jcmgh.2025.101618.

110. Waskow, C., Liu, K., Darrasse-Jèze, G., Guermonprez, P., Ginhoux, F., Merad, M., Shengelia, T., Yao, K., and Nussenzweig, M. (2008). The receptor tyrosine kinase Flt3 is required for dendritic cell development in peripheral lymphoid tissues. Nat. Immunol. *9*, 676–683. https://doi.org/10.1038/ni.1615.

111. Florez, M.A., Thatavarty, A., Le, D.T., Hill, H.A., Jeong, Y., Ho, B.M., Kus, P., Wathan, T.K., Kain, B.N., Huang, S., et al. (2024). BST2 facilitates activation of hematopoietic stem cells through ERK signaling. Exp. Hematol. *140*, 104653. https://doi.org/10.1016/j.exphem.2024.104653.

112. Laffranchi, M., Schioppa, T., Sozio, F., Piserà, A., Tiberio, L., Salvi, V., Bosisio, D., Musso, T., Sozzani, S., and Del Prete, A. (2025). Chemerin in immunity. J. Leukoc. Biol. *117*, qiae181. https://doi.org/10.1093/jleuko/qiae181.

113. Takamatsu, H., and Kumanogoh, A. (2012). Diverse roles for semaphorin-plexin signaling in the immune system. Trends Immunol. *33*, 127–135. https://doi.org/10.1016/j.it.2012.01.008.

114. Kiefel, H., Pfeifer, M., Bondong, S., Hazin, J., and Altevogt, P. (2011). Linking L1CAM-mediated signaling to NF-κB activation. Trends Mol. Med. *17*, 178–187. https://doi.org/10.1016/j.molmed.2010.11.005.

115. Loo, L., Waller, M.A., Moreno, C.L., Cole, A.J., Stella, A.O., Pop, O.-T., Jochum, A.-K., Ali, O.H., Denes, C.E., Hamoudi, Z., et al. (2023). Fibroblast-expressed LRRC15 is a receptor for SARS-CoV-2 spike and controls antiviral and antifibrotic transcriptional programs. PLoS Biol. *21*, e3001967. https://doi.org/10.1371/journal.pbio.3001967.

116. Solé-Boldo, L., Raddatz, G., Schütz, S., Mallm, J.-P., Rippe, K., Lonsdorf, A.S., Rodríguez-Paredes, M., and Lyko, F. (2020). Single-cell transcriptomes of the human skin reveal age-related loss of fibroblast priming. Commun. Biol. *3*, 188. https://doi.org/10.1038/s42003-020-0922-4.

117. Dolan, J., Walshe, K., Alsbury, S., Hokamp, K., O'Keeffe, S., Okafuji, T., Miller, S.F.C., Tear, G., and Mitchell, K.J. (2007). The extracellular leucine-rich repeat superfamily; a comparative survey and analysis of evolutionary relationships and

expression patterns. BMC Genomics *8*, 320. https://doi.org/10.1186/1471-2164-8-320.

118. Imler, J.L., and Hoffmann, J.A. (2001). Toll receptors in innate immunity. Trends Cell Biol. *11*, 304–311. https://doi.org/10.1016/s0962-8924(01)02004-9.

119. O'Prey, J., Wilkinson, S., and Ryan, K.M. (2008). Tumor antigen LRRC15 impedes adenoviral infection: implications for virus-based cancer therapy. J. Virol. *82*, 5933–5939. https://doi.org/10.1128/JVI.02273-07.

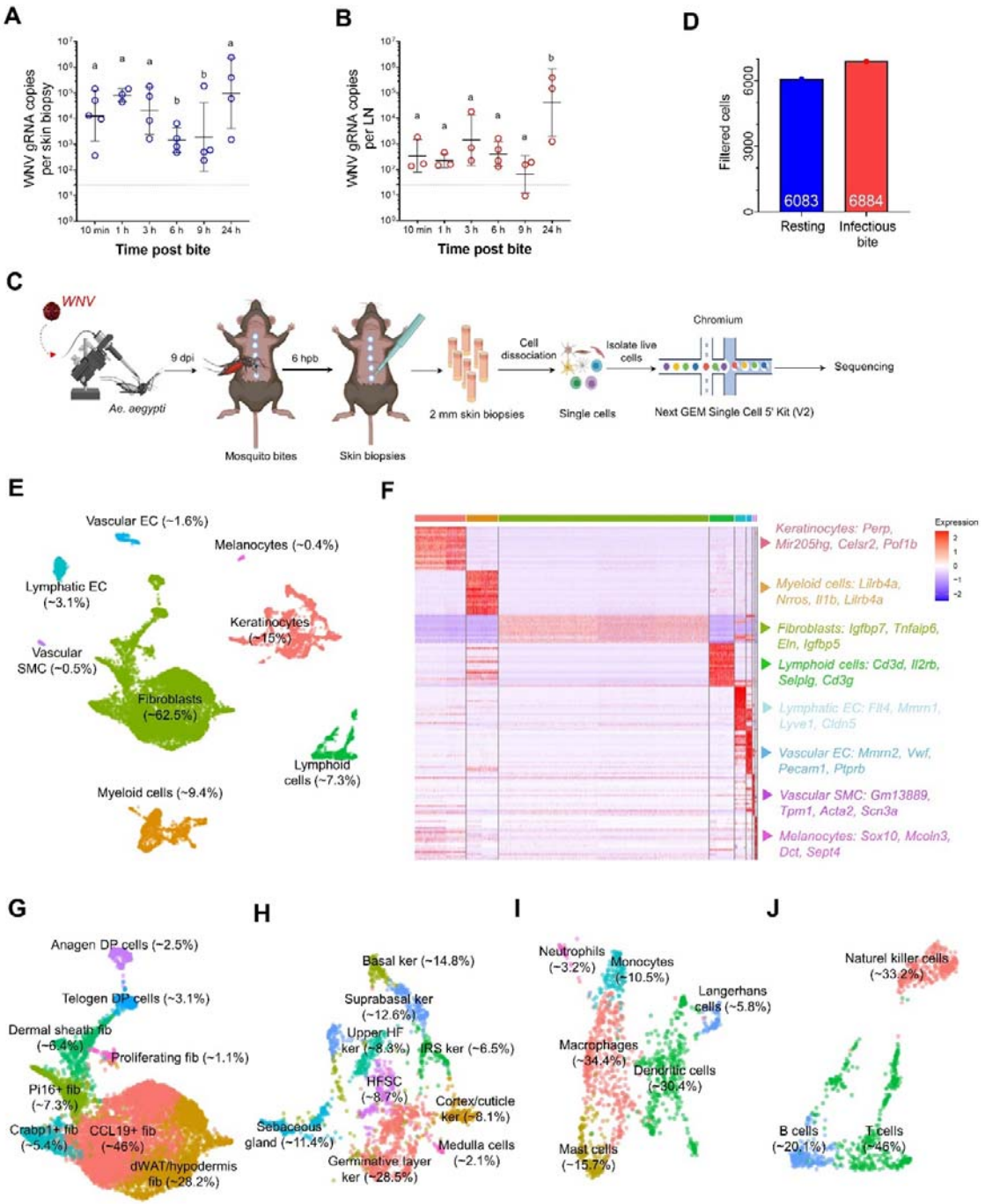

Figure 1. scRNA-seq analysis on mouse skin at the onset of bite-initiated infection

(A, B) Early WNV replication kinetics in the skin (A) and inguinal LNs of mice (B) at

10 min, 1, 3, 6, 9 and 24 hours (h) post-bite. Bars show geometric means ± 95% C.I. Point represents one skin biopsy (A) and the two inguinal LNs from the corresponding mouse (B). N mice, 3-4 per time point. Different letters indicate statistical differences as determined by post-hoc Fisher LSD's test.

(C) Experimental workflow for the scRNA-seq assay on bitten mouse skin.

(D) Numbers of high-quality single cells retained after quality control (QC) on scRNA-seq data.

(E) UMAP dimensional reduction of sequenced skin cells revealing eight cell types. Proportion of each cell cluster is provided in brackets. EC, endothelial cells; SMC, smooth muscle cells.

(F) Heatmap of the top 20 enriched genes per cell cluster. Four marker genes for each cluster are shown on the right.

(G-J) UMAP subclustering of fibroblasts (G), keratinocytes and ectodermal appendage cells (H), myeloid cells (I), and lymphoid cells (J). Relative cell proportions are indicated in brackets. Fib, fibroblasts; Ker, keratinocytes; DP, dermal papilla cells; dWAT, dermal white adipose tissue cells; HF, hair follicle cells; IRS, inner root sheath cells; HFSC, hair follicle stem cells.

See also **Figures S1-S6 and Dataset *S*1A,B; S*2*; S3**

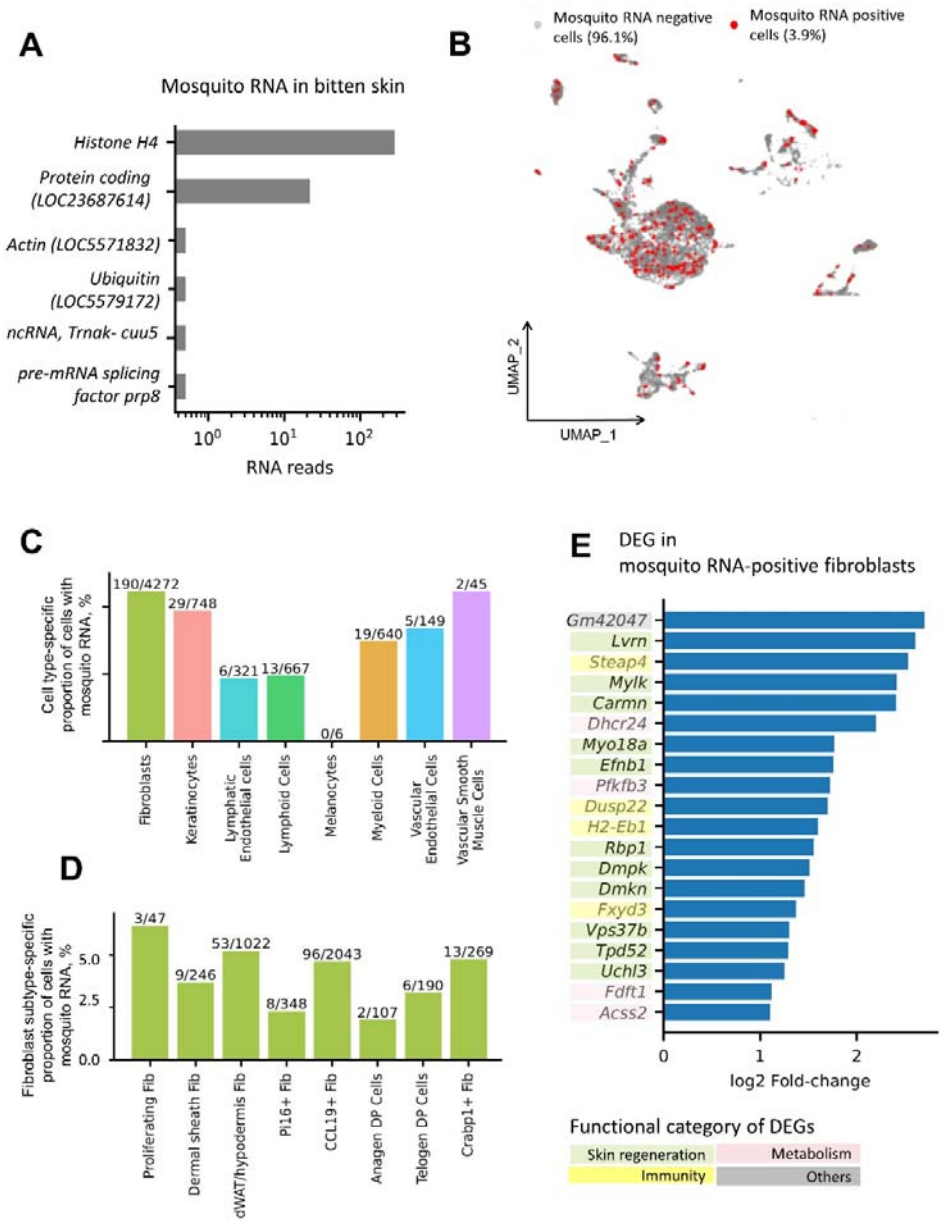

Figure 2. Cellular distribution of mosquito-derived RNAs at the cutaneous bite site

(A) Gene identification of mosquito salivary RNA fragments.

(B) Distribution of mosquito RNA-positive mouse skin cells.

(C, D) Within cell type (C) and subtype (C) proportion of mosquito RNA-positive cells. Numbers above the bars indicate absolute number of positive mouse skin cells over

total cells.

(E) Differentially expressed genes (DEG) in mosquito RNA-positive fibroblasts. Functional categories of DEGs are indicated by colored boxes.

See also **Figure S7 and Dataset S4**

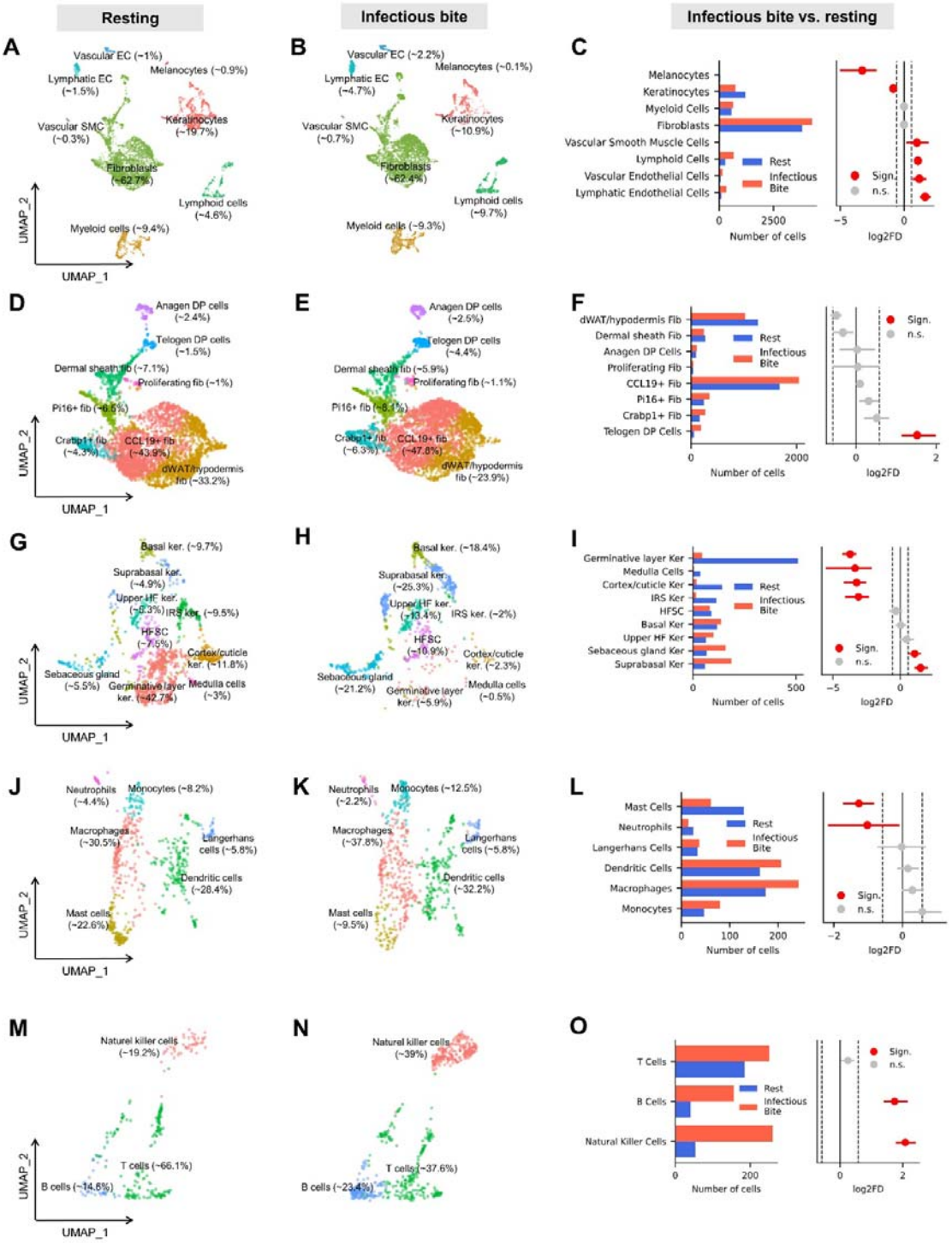

Figure 3. Cellular landscape of mouse skin after infectious bite

(A-C) Distribution of cell types in unbitten skin (i.e., rest) (A) and in the skin at 6 hours post-infectious bite (B), as well as cell number comparisons and cell type fold change

between infectious *vs.* rest conditions.

(D-O) Distribution of cell subtypes among fibroblasts (D-F), keratinocytes and ectodermal appendage cells (G-I), myeloid cells (J-L), and lymphoid cells (M-O) in unbitten skin and skin at 6 hours post-infectious bite.

(A, B, D, E, G, H, J, K, M, N) Proportions are shown in brackets. (C, F, I, L, O) Changes in cell proportions are expressed as log2 fold difference (Log2FD) means ± standard deviation in infectious bite as compared to rest conditions. Dashed black lines indicate a fold change of 1.5. Statistical significance indicated in red for $p < 0.05$ based on permutation test. ECs, endothelial cells; SMCs, smooth muscle cells; DP, dermal papilla; dWAT, dermal white adipose tissue; HF, hair follicle; IRS, inner root sheath; DCs, dendritic cells; HFSC, hair follicle stem cells.

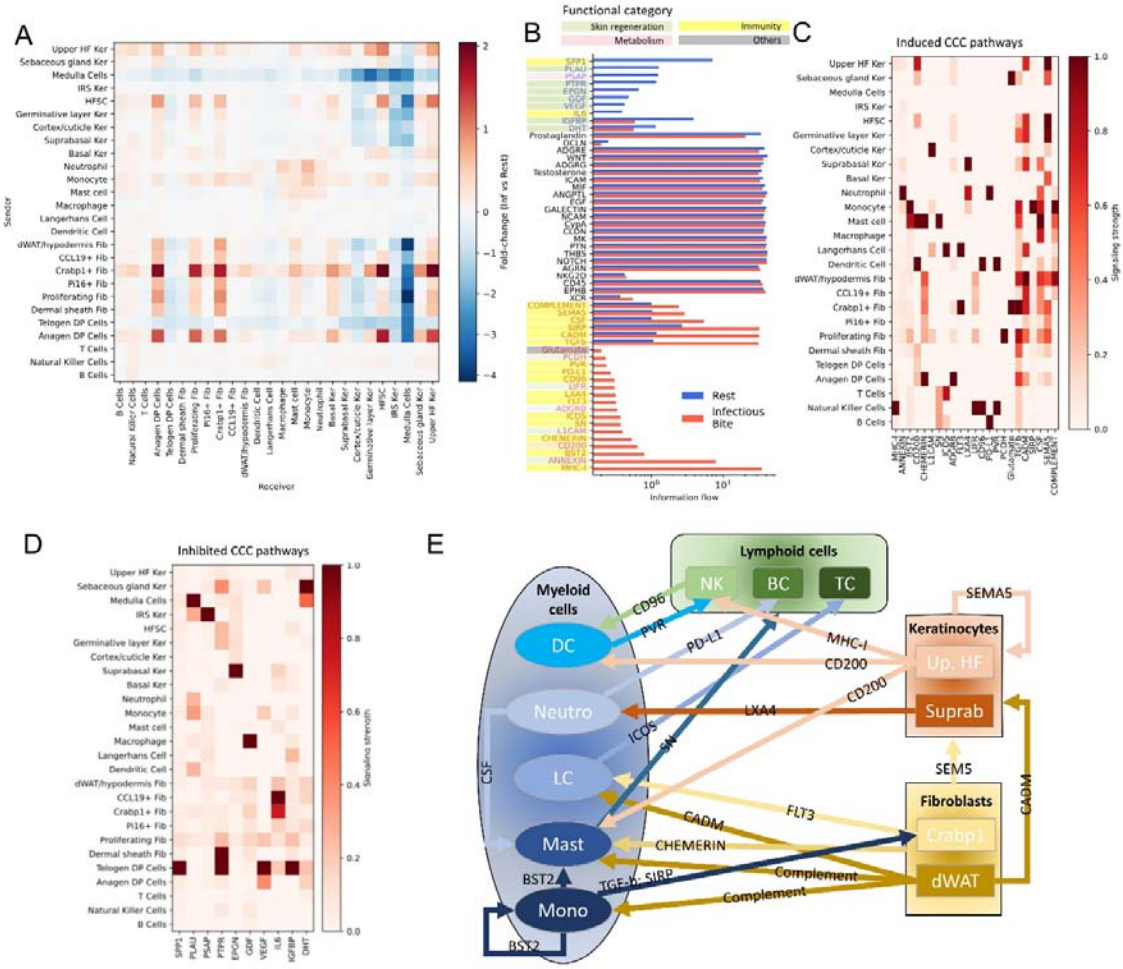

Figure 4. Cell-cell communication change in response to infectious bite

(A) Influence of infectious bite on the overall cell-cell communication (CCC) strength between skin cell subtypes. DP, dermal papilla cells; Fib, fibroblasts; Ker, keratinocytes; HFSC, hair follicle stem cells; IRS, inner root sheath cells; Up. HF, upper hair follicle cells.

(B) Pathway information flow among active CCC pathways in resting and infectious bite conditions. Pathway names in red indicate significant induction and in blue significant inhibition by infectious bite [$p < 0.001$; as determined by Wilcoxon test[86]]. Functional categories of regulated pathways are indicated by colored boxes.

(C, D) Influence of infectious bite on signaling strength for the significantly

upregulated (C) and downregulated (D) pathways per cell subtype.

(E) Overview of the upregulated CCC immune pathways.

See also **Figure S8**

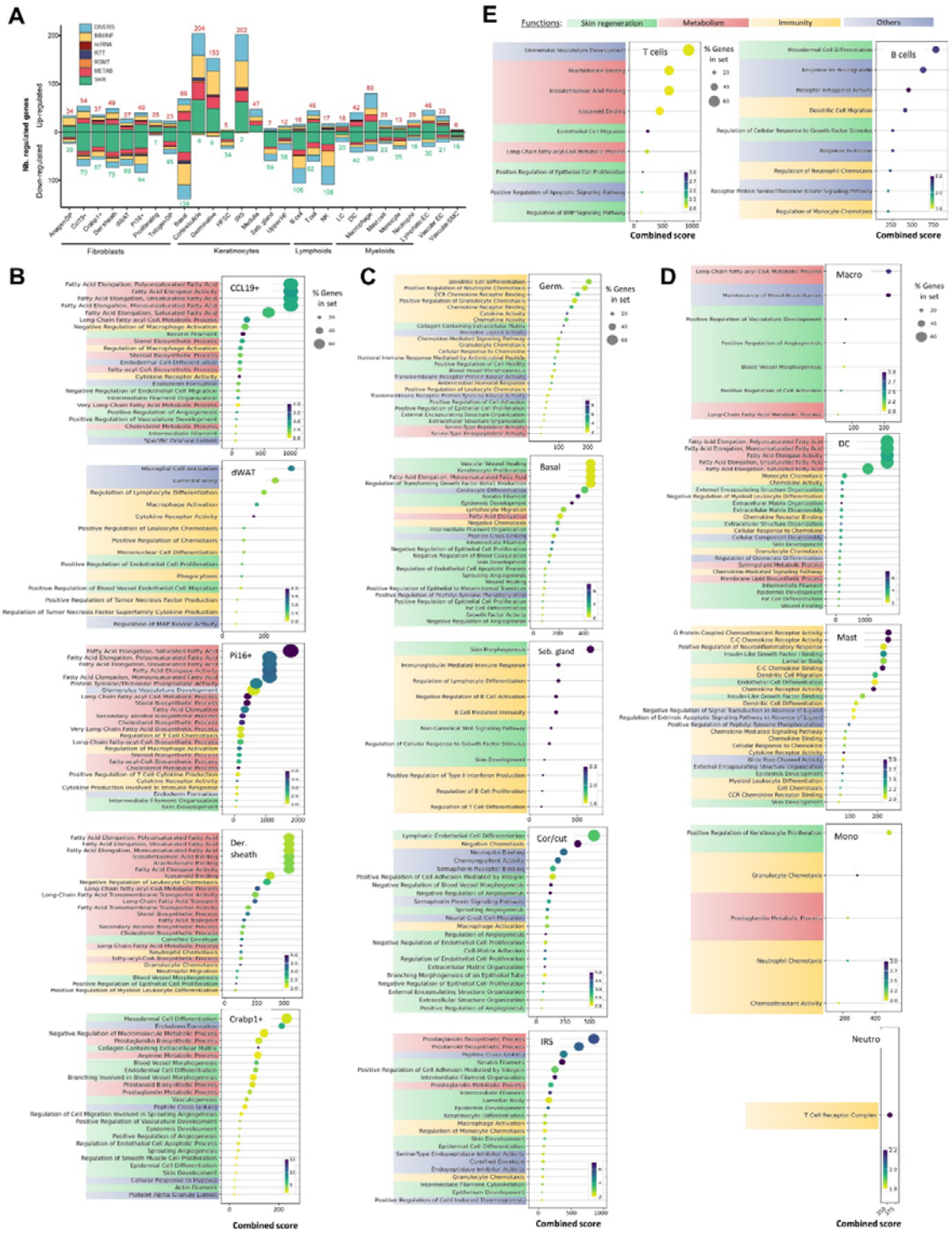

Figure 5. Cell-specific transcriptomic response to infectious bite

(A) Functional distribution of DEGs (adj. p-value < 0.001; |fold change| ≥ 4) within cell subtypes. Bars indicate the numbers of regulated genes. Functional categories: SKR,

Skin Regeneration; METAB, Metabolism; RSMT, Redox-Stress-Mitochondria; RTT, replication, transcription and translation; ncRNA, non-coding RNA; IMM/INF, immunity and inflammation; DIVERS, other and unknown functions. N total DEGs, 2,622. Number of up- and down-regulated DEGs are indicated in red and green, respectively.

(**B-E**) GO biological process enrichment analysis for top 5 most abundant subtypes of fibroblasts (B), keratinocytes and ectodermal appendage cells (C), myeloid (D) and lymphoid (E) cells. Subtypes are presented in an increasing order of abundance. Significant GO terms encompass > 10% all DEGs within subtypes and have p-value < 0.01. Subtypes not represented did not have significantly enriched GO terms. Functional categories are indicated by colored boxes. DP, dermal papilla cells; dWAT, dermal white adipose tissue cells; HFSC, hair follicle stem cells; IRS, inner root sheath cells; Seb gland, sebaceous gland cells; HF, hair follicle cells; LC, Langerhans cells; DC, dendritic cells; NK, natural killer cells; EC, endothelial cells; SMC, smooth muscle cells; Germ., germinative cells; Cor/cut, cortex/cuticle cells; Macro, macrophages; Neutro, neutrophils; Mono, monocytes.

See also **Figure S9 and Dataset S5.**

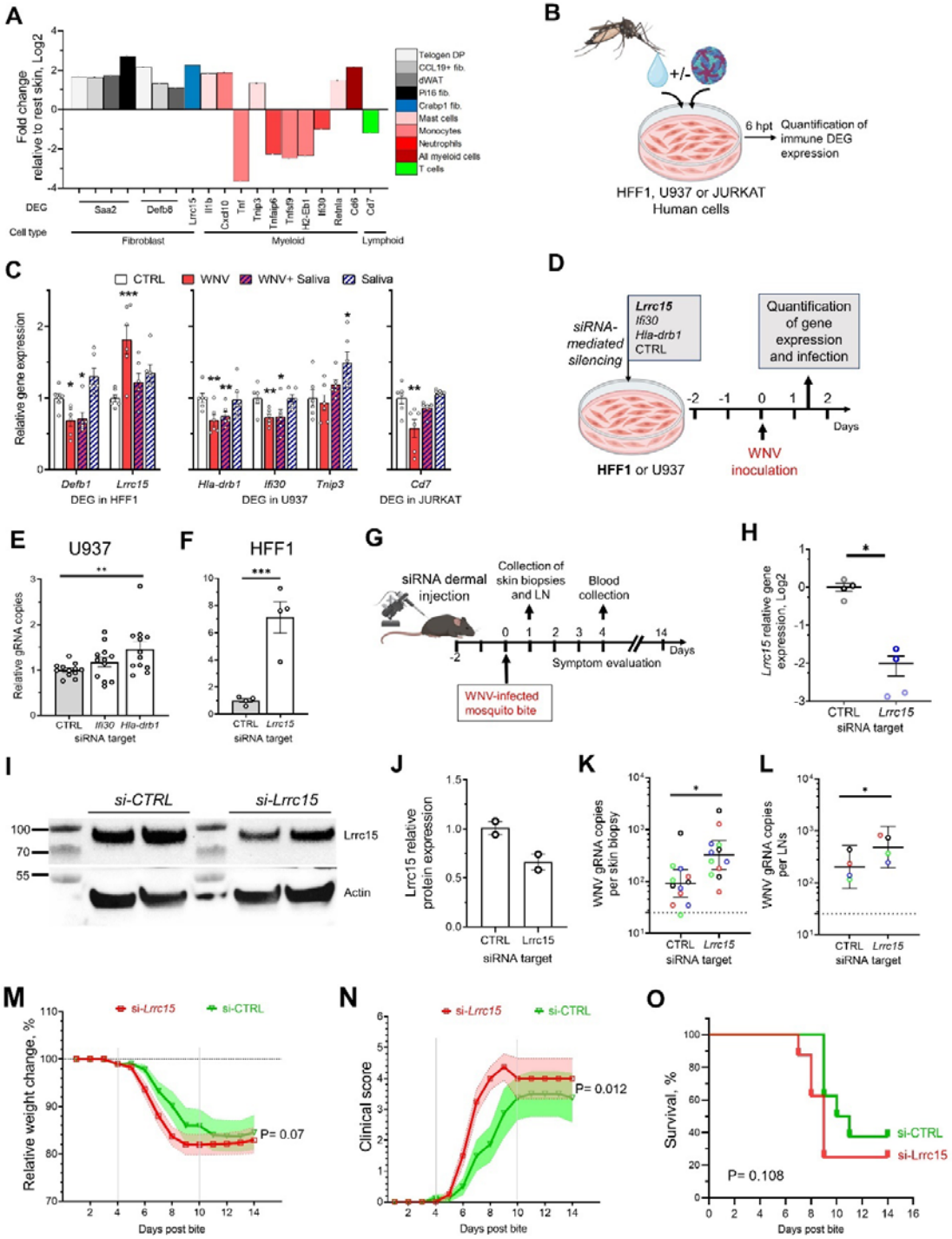

Figure 6. Fibroblast response to infectious bite reduces transmission

(A) Expression of selected immune DEGs in different fibroblast subtypes.

(B) Infection of dermal fibroblast (HFF1), monocyte (U937) or T lymphocyte (Jurkat) cells with or without mosquito saliva and quantification of selected DEGs. Hpt, hours post treatment.

(C) Regulation of DEG expressions by either saliva, virus (WNV) or both in HFF1, U937 or Jurkat cells at 6 hpt. CTRL, mock infection. DEGs that were not regulated as in skin scRNA-seq dataset are presented in Figure S11.

(D) Functional evaluation on WNV infection of DEGs in human cell lines. Lrrc15 silencing was performed in HFF1 cells, and others in U937. CTRL, siRNA control.

(E, F) Infection levels in *Ifi30*- and *Hla-drb1*-depleted U937 cells (E) and *Lrrc15*-depleted HFF1 cells (F) at 36 hours (h) post-infection.

(G) Evaluation of Lrrc15 function in transmission.

(H-J) Expression of Lrrc15 gene (H) and protein (I,J) in mouse skin at 48 h post-siRNA injection. N mice, 2.

(K, L) Infection level per skin biopsy (K) and pair of inguinal LNs (L) at 24 h post-infectious bites. N mice, 4.

(M-O) Relative weight changes (M), clinical scores (N) and survival (O) over 14 days post-infectious bite in mice intradermally injected with siRNA against *Lrrc15* or control siRNA. N mice, 8.

(C, E, F, H, J-L) Bars and lines show means ± s.e.m. Dots indicate repeats. *, $p < 0.05$; **, $p < 0.01$; ***, $p < 0.001$; by Dunett's test with CTRL or T-test. (M,N) Lines indicate mean and shaded area ± s.e.m. p, as determined by mixed-effect ANOVA for time x treatment interaction (M) and treatment effect (N). (L) p, as determined by Kaplan-Meier Survival test.

See also **Figures S10, S11 and Dataset S1, S5**